

The Fish Forestry Interaction Project – Management Model (FFIP-MM)

Preliminary Model Description and an Application
to Carnation Creek,
British Columbia

Prepared for

Dan Hogan
Ministry of Forests Research Branch
c/o Ministry of Fisheries
Fisheries Center
2204 Main Mall
University of British Columbia
V6T 1Z4

Prepared by

Clint A.D. Alexander, Timothy M. Webb, and David R. Marmorek

ESSA Technologies Ltd.
Suite 300, 1765 West 8th Avenue
Vancouver, BC V6J 5C6

Lookfar Solutions
Tofino, BC

September 25, 1998

Citation for original document:

Alexander, C.A.D., T.M. Webb and D.R. Marmorek. 1998. The Fish Forestry Interaction Project – Management Model (FFIP-MM): Preliminary Model Description and an Application to Carnation Creek, British Columbia. Prepared by ESSA Technologies Ltd., Vancouver, BC, and Lookfar Solutions, Tofino, BC. 50 pp.

© 1998 ESSA Technologies Ltd.

No part of this publication may be reproduced, stored in a retrieval system, or transmitted, in any form or by any means - electronic, mechanical, photocopying, recording, or otherwise - without prior written permission from ESSA Technologies Ltd., Vancouver, BC.

Acknowledgments

This model was developed with the expertise and enthusiastic participation of a wide diversity of scientists with expertise in fish-forestry interactions (Table 1), who contributed during two structured workshops and three technical meetings. We thank the scientific authorities, Dan Hogan and Steve Chatwin, BC Ministry of Forests, Research Branch for their enthusiasm and guidance through all stages of the project. We also thank the members of the Scientific Review Committee for their comments on the design of FFIP-MM. The project was implemented by a team from ESSA Technologies Ltd. and Lookfar Solutions Inc.. David Marmorek (ESSA) managed the project while Clint Alexander (ESSA) led model development in co-operation with Tim Webb from Lookfar Solutions.

Table 1: Participants in FFIP-MM. “c” = participant most closely associated with channel submodel; “u” = participant most closely associated with the upslope submodel; and “f” = participant most closely associated with the fish habitat submodel.

Name	Affiliation
Steve Chatwin ^{u,c}	Ministry of Forests
Dan Hogan ^c	Ministry of Forests
Michael Church ^c	University of British Columbia, Department of Geography
Jonathan Fannin ^u	University of British Columbia, Civil Engineering
Terry Rollerson ^u	Ministry of Forests
Mike Wise ^u	Ministry of Forests
Roy Sidle ^u	University of British Columbia, Department of ???
Peter Tschaplinski ^f	Ministry of Forests
Derek Tripp ^f	Consultant
Bruce Ward ^f	Ministry of Environment Lands and Parks
Dave Bustard ^f	Consultant
Dave Tredger ^f	MELP
Josh Korman ^f	Consultant, Ecometric
? Dale	Consultant
? Decker	Consultant

Funding for this research project was provided by Forest Renewal BC.

Cautionary Note

The results presented in this report do not represent a rigorous retrospective analysis of the effects of logging in Carnation Creek on salmonid habitat. The main purpose of this report is to demonstrate the analysis capabilities of FFIP-MM now that the prototype is complete. Future work will be required to refine model parameters and expert rules, compare model outputs to historical data on landscape location and frequency, and to define alternative management scenarios. Nevertheless, by examining model behaviour in relation to historical impacts of logging in Carnation Creek for a *preliminary* set of rules and parameters, this report initiates the first step in a more formal evaluation strategy. This evaluation strategy requires further participation by FFIP-MM participants.

Table of Contents

List of Tables	iv
List of Figures.....	v
1.0 Introduction.....	1
2.0 Methods.....	3
2.1 <i>Data Requirements</i>	3
2.2 <i>Simulation Model</i>	3
2.2.1 Calibration.....	7
2.2.2 Initialization	8
2.2.3 Hydrology submodel	10
2.2.4 Upslope submodel.....	10
2.2.4.1 Management scenarios	10
2.2.4.2 Forest Growth.....	11
2.2.4.3 Debris slide travel distance.....	11
2.2.5 Channel submodel.....	13
2.2.6 Habitat capability submodel.....	17
3.0 Preliminary Results and Discussion	20
3.1 <i>Calibration</i>	20
3.2 <i>Upslope submodel</i>	22
3.3 <i>Channel submodel</i>	26
3.3.1 Watershed Wide Results	26
3.3.2 Results for Select Reaches	28
3.4 <i>Habitat capability submodel</i>	36
4.0 Conclusion and Recommendations.....	41
5.0 References.....	42
Appendix A: Parameter Values Used in the Simulations	43

List of Tables

Table 1:	FFIP-MM Spatial Data Requirements.	3
Table 2:	FFIP-MM External Data Requirements.....	3
Table 3:	FFIP-MM “looking outward” matrix showing the major components of the model and their linkages..	5
Table 3:	Pristine and initial CAP states assumed in the test application of FFIP-MM to Carnation Creek.....	9
Table A1:	Riparian Tree Fall parameters.	43
Table A2:	Proportion of reach volume storing LWD in steady state (equilibrium).....	43
Table A3:	Proportion of reach volume storing coarse sediment in steady state (equilibrium).	43
Table A4:	Volume of sediment stored by LWD (Γ).....	43
Table A5:	Stand growth parameters as a function of site index.	44
Table A6:	Downed LWD dynamics.	44
Table A7:	Slope failure hazard classification	44
Table A8:	Slope failure probability parameters.....	45
Table A9:	Initial slide volume (V_{init}) parameters for four terrain classes.	45
Table A10:	Proportion of LWD entrained by debris slides of different magnitudes.....	45
Table A11:	Total slide volumes corresponding to “small”, “medium”, and “large” magnitude failure events.....	46
Table A12:	Multipliers used to derive bank input volumes of sediment in aggrading reaches	46

List of Figures

Figure 1:	Generalized flow-chart for FFIP-MM.	6
Figure 2:	Volumetric modelling framework (adapted from Wise 1997).....	12
Figure 3:	Reaches used in the test application of FFIP-MM to Carnation Creek.....	14
Figure 4:	Generalized channel submodel flow-chart.....	16
Figure 5:	Results of an expert elicitation of the habitat capability value of different CAP type and states for coho salmon.	19
Figure 6:	Debris slide history for a 1000 year simulation of Carnation Creek in the ‘pristine’ condition	20
Figure 7:	Calibration results.....	21
Figure 8:	Simulated mean number of stream impacting slides between 1950 to 2100	22
Figure 9:	Simulated mean probability of slope failure between 1950 to 2100.....	23
Figure 10a:	Road and cut block locations (forest age structure) in 1980.....	24
Figure 10b:	Road and cut block locations (forest age structure) in 1991.....	25
Figure 11:	Simulated watershed wide trends in sediment and LWD storage volumes.	27
Figure 12:	Average watershed wide volume of LWD simulated by FFIP-MM in comparison with the observed mean volumes of LWD for 86 streams surveyed throughout the Pacific Northwest	28
Figure 13:	Simulated average annual landslide inputs of sediment from 1950 to 2060 in three different regions of Carnation Creek.	29
Figure 14:	Simulated average annual landslide inputs of LWD from 1950 to 2060 in three different regions of Carnation Creek.	30
Figure 15:	Simulated average annual riparian inputs of LWD from 1950 to 2060 in three different regions of Carnation Creek.	31
Figure 16:	Simulated average sediment storage volumes from 1950 to 2060 in three different regions of Carnation Creek.	32
Figure 17:	Simulated average LWD storage volumes from 1950 to 2060 in three different regions of Carnation Creek.	33
Figure 18:	Simulated average sediment storage volumes from 1950 to 2000 for reach 5 under pristine conditions (green line) and historical logging (red line).	34
Figure 19 (next page):	Simulated average CAP from 1950 to 2060 (historical logging) for select reaches under pristine conditions and historical logging	34
Figure 20:	Simulated average WHC values for coho spawning in Carnation Creek under pristine conditions and historical logging activities	36
Figure 21:	Simulated average WHC values for coho rearing in Carnation Creek under pristine conditions and historical logging activities.	37
Figure 22:	Simulated average WHC values for coho overwintering in Carnation Creek under pristine conditions and historical logging activities.	37
Figure 23:	Monte Carlo probability distributions of CAP state for lower mainstem reaches 1, 5, and 9 under pristine conditions and current parameter values.....	38
Figure 24:	Mean simulated WHC rating for coho summer rearing under historical logging and pristine conditions (70 Monte Carlo trials).....	39

1.0 Introduction

The Fish Forestry Interaction Program (FFIP) was initiated in 1981 to study the problem of the effects of mass wasting of soils in steep coastal watersheds on fish habitat. FFIP research was given a high priority as an increasing proportion of coastal harvesting was occurring in middle and upper slopes of British Columbian (BC) watersheds with moderate to high slope stability problems. Since 1981, researchers from government, universities, the private sector, and industry have been working cooperatively to develop tools that allow forestry and fisheries values to be integrated into watershed planning and management. FFIP research has contributed to a greater understanding of various physical and biological processes affected by forestry-related development. This progress is documented in more than 50 BC Ministry of Forests Land Management Reports, numerous publications in the peer-reviewed literature, in several BC Forest Practices Code Guidebooks, and a number of workshop reports.

Despite the above progress, there was no management focused tool that linked upslope forest harvesting impacts, sediment and large woody debris (LWD¹) transport processes, and site specific impacts on fish habitat. The first major step in providing this linkage occurred in 1991 when members of ESSA Technologies helped 20 scientists from government, industry, and university to develop a detailed mechanistic model of fish forestry interactions. This model, the Fish Forestry Interaction Program Simulation model (FFIPS), focused on simulating changes in channel morphology and dynamics² because it was the most technically uncertain and challenging part of the overall system. Though much was learned, the modelling exercise taught those participating that their level of understanding of the variables and processes governing changes in channel morphology was insufficient to develop a detailed mechanistic model. In short, more basic research was needed. While this model continues to be used as a research tool at the University of British Columbia, forestry managers indicated that what was required was a more operational level planning tool built upon more routinely collected data.

Interest in a simpler management-oriented model prompted a two-day workshop in December 1996 to explore design options and feasibility. That workshop, along with another workshop in November 1997 and several subsequent technical meetings generated the blue print for the prototype fish-forestry interaction model presented in this paper — FFIP-MM. With the thoughtful contributions of these scientists (Table 1) and the direction of Steve Chatwin and Dan Hogan from the Ministry of Forests, ESSA has completed the development of this model.

FFIP-MM is a prototype management tool for coastal watersheds. Its purpose is to link upslope forest harvesting activities to changes in stream sediment and large woody debris (LWD) transport processes. The rate and magnitude of delivery of LWD and sediment from hillslopes is then related to reach specific impacts for several fish species based on an expert assessment of habitat capability (fresh water survival and productivity) for the 49 different stream morphologies and disturbance states defined under the Channel Assessment Procedure (CAP) of the BC Forest Practices Code; (BC Ministry of Environment, 1996).

¹ In FFIP-MM, the terms: Larger Organic Debris (LOD) and LWD were used interchangeably, however LWD is the preferred term.

² e.g., simulating reach by reach: substrate composition, moveable bedload, bar storage of gravel, number of log jams by age class, area and depth of pools, ratio of channel to riffle area, density of fine organic matter, percent area of undercut bank, etc.

The model can answer questions like:

- \$ What are the reach specific and cumulative watershed impacts on fish habitat of timber harvesting?
- \$ How likely are debris slides to be transmitted from one part of the watershed to another?
- \$ How long will it take for the watershed to recover from a particular intensity of harvesting?

Uses of FFIP-MM include:

- \$ assess the range of possible impacts of logging plans on fish habitat capability;
- \$ a tool for teaching fish-forestry linkages;
- \$ a tool for communication and increasing scientific understanding;
- \$ assisting in the design of research experiments; and
- \$ aiding in prioritization of inventory efforts.

This report reviews this model's structure and presents some preliminary results for an application of FFIP-MM to the Carnation Creek watershed. The preliminary model results are compared with the summary of Carnation Creek logging impacts presented in Hartman et al. (1996). A brief discussion then focuses on similarities and discrepancies between the observed and modelled trends. Readers interested in model details not covered in this report should obtain a copy of the FFIP-MM User's Guide by contacting Dan Hogan, Ministry of Forests Research Branch (604 - 222 - 6752).

2.0 Methods

2.1 Data Requirements

FFIP-MM uses GIS software to obtain grid representations of the required spatial information (see ESSA 1998 for details). Additional information for these spatial elements is provided in an external database. The spatial information needed to apply the model to a given watershed is given in Table 1, along with external data requirements in Table 2.

Table 1: FFIP-MM Spatial Data Requirements.

Spatial Information
Elevation (m)
Stream reach locations and ID
Gully locations
Logging road locations and the year of construction
Slope stability class (I-V); (BC Ministry of Environment 1995)
Forest Cover polygon locations and ID

Table 2: FFIP-MM External Data Requirements.

Forest Cover Information (by stand)		Stream Reach Information	
	<i>Description</i>		<i>Description</i>
Most recent or scheduled year of harvest	Age at which a given polygon is harvested (1 rotation only).	Average length (m)	Length of each given reach in metres.
Mean stand age	Stand age in the reference year.	Average width (m)	Width of each given reach in metres.
Reference year	Year age structure inventory performed	Average depth (m)	Depth of each given reach in metres.
Site index	An expression of the forest site quality based on stand age and height. Site index is determined using stand age, stand height and Ministry of Forests' and other site index equations. These equations are based on reference age 50 years bha (Breast Height Age).	Equilibrium CAP type	CAP type in dynamic equilibrium.
		Initial CAP state	CAP state in the year you wish to start the simulation.
		Pristine CAP state	CAP state in dynamic equilibrium
		Downstream Reach ID	Determines what reach receives upstream LOD and sediment inputs

2.2 Simulation Model

FFIP-MM has three major components: 1) an Upslope submodel that simulates the probability of slope failure and downslope propagation of sediment and LWD; 2) a Channel submodel describing the sediment storage capacity of each reach, and the rate of movement of sediment and LWD through the drainage network; and 3) a Fish Habitat submodel relating the storage of sediment and LWD to an expert rating of habitat value based on CAP (BC Ministry of Environment 1996). The model accounts for

uncertainty in both spatial and temporal components (e.g. where landslides occur; the severity of storm events in a given year). Using Monte Carlo simulation, the model produces probability distributions for fish habitat ratings on a spatially explicit basis through time. These calculations use both explicit physical relationships based on empirical data (e.g. regressions to estimate changes in slide volume based on slope and other variables), as well as expert rules (e.g. proportion standing and downed timber entrained by debris slides). Since expert rules predominate, FFIP-MM is best described as a spatially explicit, quasi-empirical expert system.

A generalized flow-chart of the model (Figure 1) indicates its major components while Table 3 summarizes the connections between these elements. Submodel details are described below. In general, FFIP-MM completes the following general steps:

1. The model is calibrated by running the Upslope submodel under ‘pristine’ old-growth conditions to determine the average annual inputs of LWD and sediment from debris slides to each stream reach.
2. Next, the model determines the initial forest age structure, harvest schedule, and reach specific CAP types and states. Based on the results of Step 1, FFIP-MM then calculates the equilibrium (steady state) LWD and sediment loss rates for each reach.
3. The model simulates debris slide initiation, routing, volume, and composition for events initiating on four General Terrain Classes (hereafter GTC): old-growth terrain, clear-cut terrain, gullies, and roadbeds.
4. The channel submodel then establishes a mass balance for LWD and sediment within the watershed’s individual stream reaches, and annually updates CAP state (not morphology, which remains consistent) based on the proportion of the reach’s volume storing sediment.
5. Finally, the habitat capability of each reach is calculated for several salmonid species and life-stages. These ratings are based on an expert assessment of the habitat capability of the 49 different CAP type and state combinations.
6. The individual ratings for the watershed’s reaches are then converted into a watershed habitat capability rating (hereafter WHC).

These steps can be repeated for alternative logging plans to determine the probability distribution for possible WHC outcomes. Details of these various components follow.

Table 3: FFIP-MM “looking outward” matrix showing the major components of the model and their linkages.

From	To	Upslope	Channel	Fish habitat
Upslope		X	<ul style="list-style-type: none"> • Index of annual peak storm flow intensity • Volume of SED and LWD delivered to each reach 	—
Channel		—	X	<ul style="list-style-type: none"> • CAP state
Fish habitat		—	—	X
Management Actions	<ul style="list-style-type: none"> • Areas harvested • Timing of harvest • Road locations 		—	—
Driving Variables	<ul style="list-style-type: none"> • Slope stability class • Terrain class (e.g. road, clear-cut, old-growth, gully) • Time since harvest / road construction • Initial slide volume • Slope angle • Slide width • Slide depth • Live stand volume • Downed LWD volume 		<ul style="list-style-type: none"> • Natural SED and LWD input rates • Variation in stream flows • SED stored by LWD • LWD decay rate 	<ul style="list-style-type: none"> • CAP type • CAP state • Reach length • Expert rankings of CAP habitat capability as a f(species, life stage)

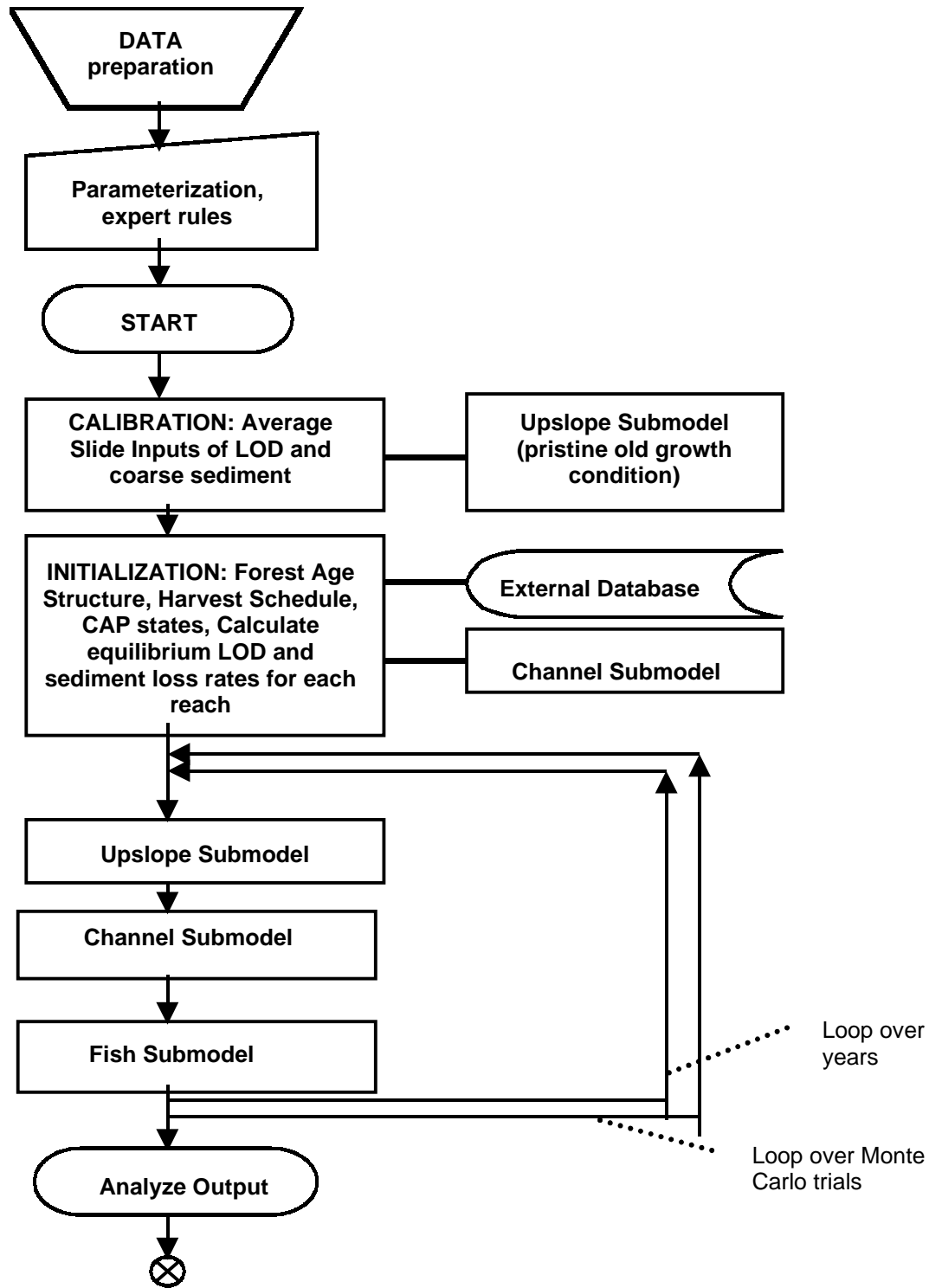


Figure 1: Generalized flow-chart for FFIP-MM.

2.2.1 Calibration

The average annual inputs of LWD and sediment from debris slides are determined during a one-time calibration step.³ FFIP-MM uses these values along with reach specific initialization information to calculate the annual loss rates for LWD and sediment for each reach. These calculations are shown in equations [1] and [2]:

$$\mathbf{FL}_{e,r} = \{ \sum \text{LWD Inputs}_{e,r} - (\sum \text{LWD Inputs}_{e,r} - \text{LWD}_{e,r}) \times \kappa \} / \{ (\sum \text{LWD Inputs}_{e,r} + \text{LWD}_{e,r}) \times (1 - \kappa) \} \dots \text{ [1]}$$

where;

- \$ $\mathbf{FL}_{e,r}$ is the average annual proportion of LWD “flushed” out of reach r in an equilibrium (e) steady state;
- \$ $\text{LWD Inputs}_{e,r}$ is the annual equilibrium input of LWD to reach r from upstream reaches, riparian tree fall (see Appendix A), and landslides (in m^3);
- \$ $\text{LWD}_{e,r}$ is the equilibrium storage volume (m^3) of large woody debris for reach r 's CAP morphology and pristine CAP state (obtained via linear interpolation using the data in Table A2, Appendix A); and
- \$ κ is the annual proportion of LWD lost to the atmosphere through natural decay.

$$\mathbf{FS}_{e,r} = \sum \text{Sediment Inputs}_{e,r} / \{ \sum \text{Sediment Inputs}_{e,r} + (\text{Sediment Capacity}_{e,r} - \Gamma_{e,r}) \} \text{ [2]}$$

where;

- \$ $\mathbf{FS}_{e,r}$ is the average annual proportion of coarse sediment ($> 3\text{mm}$) “flushed” out of reach r in the steady state;
- \$ $\text{Sediment Inputs}_{e,r}$ is the annual equilibrium input of sediment to reach r from upstream reaches and landslides⁴ (in m^3);
- \$ $\text{Sediment Capacity}_{e,r}$ is the equilibrium storage volume (m^3) of sediment for reach r 's CAP morphology and pristine CAP state (obtained via linear interpolation using the data in Table A3, Appendix A); and
- \$ Γ is the volume (m^3) of sediment stored by $\text{LWD}_{e,r}$ for reach r 's CAP morphology and pristine CAP state (see Table A4, Appendix A).

During a simulation, the calibrated values of FL and FS become state variables that are modified by a random variable representing natural variation in precipitation and run-off (i.e. an annual peak flow intensity index).

This mass balance formulation for the channel submodel presumes the major source of sediment supplied to stream channels derives from mass wasting events (debris flows and slides on open slopes and in gullies). Because FFIP-MM does not track fine sediments, the model assumes that fine sediments ($< 3\text{mm}$) pose an insignificant hazard to fish habitat capability in high-energy coastal watersheds like Carnation Creek.

³ This calibration must be repeated if model parameters are changed.

⁴ sediment input from bank erosion is assumed to be negligible in steady state.

2.2.2 Initialization

The harvest schedule, forest age structure, pristine and initial CAP states, and the CAP morphology of each reach are determined during initialization. Table 3 gives the pristine and initial CAP state values used in the test application of FFIP-MM to Carnation Creek.

Table 3: Pristine and initial CAP states assumed in the test application of FFIP-MM to Carnation Creek. Figure 3 provides the spatial locations and relative sizes of these 47 reaches.

Reach	Pristine CAP state	Initial CAP state
1	S	S
2	S	A1
3	S	A1
4	D1	D1
5	A1	A1
6	A1	A1
7	A1	D1
8	D1	D1
9	S	A1
10	S	A1
11	S	S
12	S	S
13	S	S
14	S	S
15	S	A1
16	S	S
17	D2	S
18	S	A1
19	S	S
20	S	S
21	S	D1
22	S	S
23	A1	A1
24	A1	A1
25	S	S
26	D1	S
27	S	A1
28	D1	S
29	S	A1
30	S	A1
31	S	S
32	S	S
33	D2	S
34	S	S
35	S	A1
36	S	S
37	D2	S
38	S	S
39	S	S
40	D1	S
41	S	S
42	A1	S
43	S	S
44	D1	S
45	D2	S
46	S	S
47	D2	S

2.2.3 Hydrology submodel

The FFIP-MM prototype does not use a process-based model of the impacts of logging on watershed hydrology and stream run-off. Instead, hydrological variation is taken into account implicitly using a log-normal probability distribution to represent an index of annual variation in the intensity of fall/winter storm events. The resultant random variable is used in the upslope submodel as a modifier to the probability of slope failure, and by the channel submodel to increase or decrease the annual loss rate for sediment ($FS_{e,r}$, equation 2). Because LWD is less mobile than sediment, a separate log-normal distribution with lower variance was applied to the annual LWD loss rate ($FL_{e,r}$, equation 1). The choice of a log-normal distribution was based on the observed distribution of long-term precipitation and stream flow patterns in coastal watersheds like those in the Queen Charlotte Islands (Hogan and Schwab 1990). However, the parameters used for these distributions (mean of 1 and a SD of 0.25 for the upslope index, but a SD of 0.1 for the index of LWD flushing variability) were subjective. Empirical parameterization is difficult because the multipliers are applied to the loss rates of LWD and sediment, not specific, routinely measured quantities like the maximum instantaneous winter discharge. Refinement of this parameter could be completed by comparisons with more detailed hydrology models.

A notable limitation with this method of modelling variation in fall/winter storm flows is that it does not consider the increase in water yield that is observed to occur downstream of large logged areas (Hartman *et al.* 1996), nor does it consider longer-term cyclic trends in precipitation and climate patterns. These limitations could easily be overcome in future versions of the model.

2.2.4 Upslope submodel

The upslope submodel is responsible for simulating stand growth and decay, the probability of slope failure, and upon a slope failure event - the travel distance and magnitude of the resultant debris slide/flow/torrent (hereafter just debris slide or landslide for simplicity). Forest harvesting scenarios (the location and rate of cut) are implemented within the upslope submodel as modifiers to the probability of slope failure and debris slide magnitude. Details are discussed in the next three sections.

2.2.4.1 Management scenarios

This report describes preliminary results for two alternative scenarios. First, to ensure that the model was internally consistent, a “pristine” simulation was performed from 1900 to 1950 (no logging or natural disturbances). Second, the model was then run according to the historical roading and logging plan in Carnation Creek from 1967 to 1994. For the historical logging scenario, the simulation was conducted from 1950 to the year 2100 to ascertain the approximate rate of habitat capability recovery following a large-scale clear-cut logging operation. Here too the effects of natural disturbances were not considered.

In general, the management actions supported by the prototype model are:

- \$ areas harvested;
- \$ rate of harvest; and
- \$ road location.

GIS software is used to design the spatial layout of the harvesting plan when considering other scenarios, with the order and rate of cut defined in an external database (see ESSA 1998 for details).

2.2.4.2 Forest Growth

In FFIP-MM, forest stands are viewed as a volume of standing (live) and downed (dead) LWD along a potential debris slide path. Both standing and downed volumes were a function of stand age and site index according to a series of standard signroid shaped relationships (Table A5, Appendix A). Downed LWD was assumed to accumulate as a fixed proportion of the live volume of the stand, less natural decay. Upon harvesting a stand, a proportion of the live volume was immediately added to the “dead pool” (Table A6, Appendix A). These volume over age relationships are parameterized from the point of view of average volumes growing in particular bio-geoclimatic zone, and not on a species by species basis.

2.2.4.3 Debris slide travel distance

To model slope failure probability and debris travel distance, FFIP-MM divides the watershed into four general terrain classes (GTC): old growth (not previously harvested), clear-cut, gullies, and roads. These four GTC’s were then further stratified by slope stability class (BC Ministry of Environment 1995), and for clear-cuts and roads, by their age. Terrain was then assigned a qualitative slope failure hazard designation of very low, low, medium, high, or very high. With the storm intensity index now serving as the predictor variable, the five slope failure hazard classes are then assigned to a family of curves defining the average probability of slope failure per hectare per year (see ESSA 1998). These probabilities are based on expert judgment and wherever possible calibrated to observed landslide frequencies (e.g., BC Ministry of Environment 1995). As a general rule, the probability of slope failure at the median value of the distribution used to represent storm intensity should be set to match long-term slope failure frequencies for the GTC in question.

To determine the probability of slope failure, the model randomly loops over grid cells, ascertaining their GTC, slope stability class, and if necessary, the age of the road or clear-cut, and then applies the log-normal random variable representing storm intensity. A uniform random number between 0 and 1 is then drawn to determine whether a failure occurs. Tables A7 and A8 in Appendix A provide the slope failure hazard class and probability parameters used in the test application to Carnation Creek.

Once a slope failure occurs, a modified version of the volumetric modelling approach described by Wise (1997) was used (Figure 2). In brief, Wise (1997) used data from 131 debris flow events occurring on 6 to 15 year post-clear cut terrain in the Queen Charlotte Islands⁵ to develop a series of volumetric multiple regression equations. The regression equations were developed by using field measurements of the length, width of scour and/or deposition, depth of scour and/or deposition, and the slope angle and path azimuth of these 131 debris slide events. These empirical relationships were developed separately for open ground, unconfined slope morphologies, and gully (confined) morphologies (Wise 1997). The field observations suggested, and these equations predict entrainment of material on steeper portions of the slope, which increases flow volume, while lower gradient terrain causes deposition that reduces the cumulative flow volume (Wise 1997).

⁵ Methodology used to map these events described in Rollerson (1992).

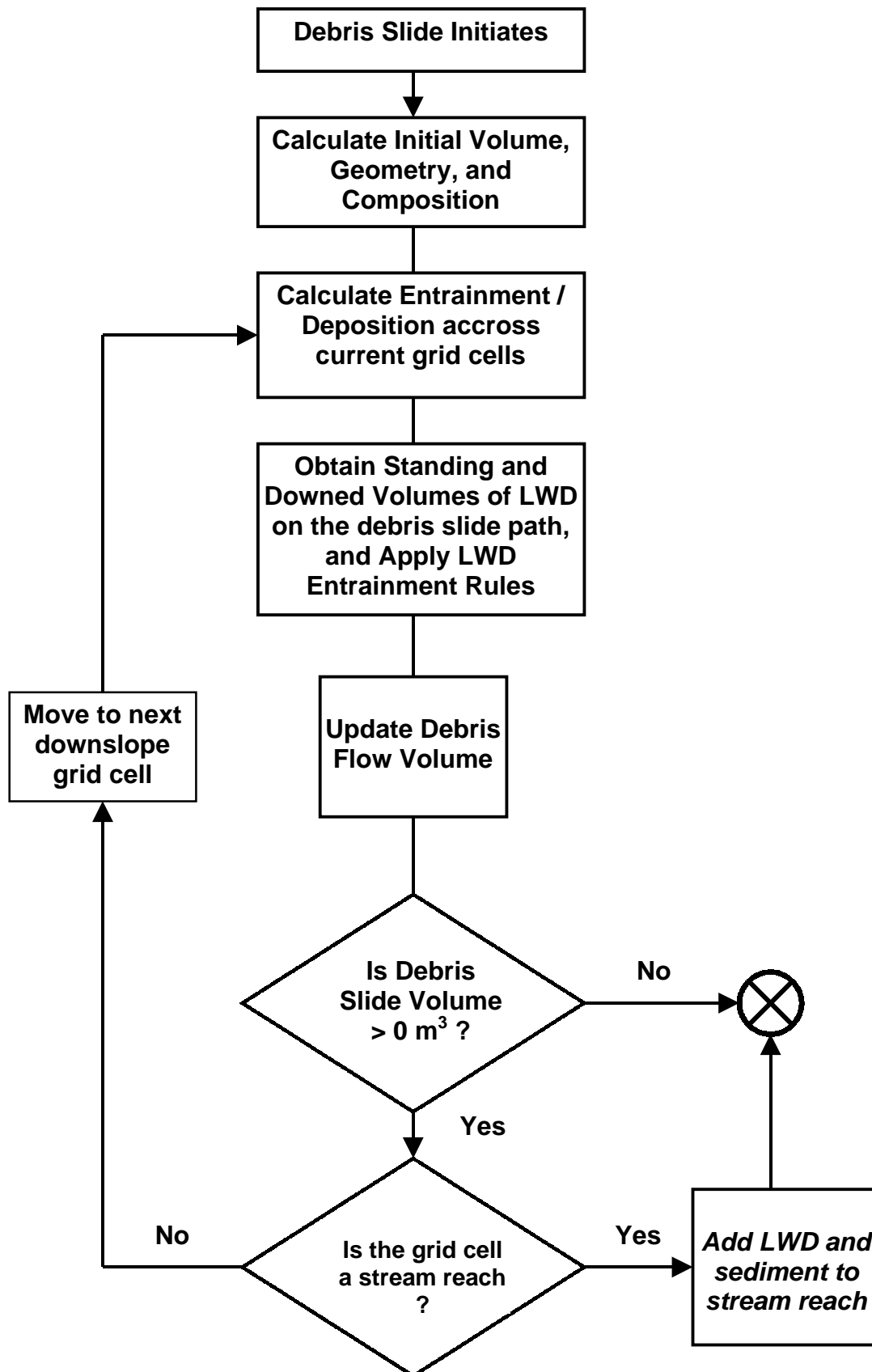


Figure 2: Volumetric modelling framework (adapted from Wise 1997).

Because FFIP-MM *simulates* debris slides (rather than “plugging in” data for specific surveyed events), we needed to make several modifications to the volumetric modelling framework given in Wise (1997). First, the initial slide volume (Vinit) had to be determined. This was done in a manner equivalent to that used to calculate slope failure probabilities. With the random variable for annual storm intensity again serving as the independent variable, four curves for each GTC were assigned to calculate Vinit. Thus, larger storms tended to produce larger initial slide volumes, with less intense storm years producing smaller events. Parameterization of these functions (see Table A9, Appendix A) for clear-cuts, roads, and gullies was based on the distributions of Vinit given in Wise (1997). However, the parameters for Vinit for events occurring on old growth terrain were based on expert judgment. The initial slide material was assumed to be composed of coarse sediment (55%), fine sediment (15%), and fine organic material (30%). The second modification made to the volumetric modelling framework in Wise (1997) was the need to determine the initial geometry of the slide, namely the slide depth and width. This was done by stochastically generating a slide depth from a $N[0,0.5]$ normal distribution, and then assigning the slide width by simply dividing Vinit by the product of the slide depth and the length of the hypotenuse between the current grid cell and its lowest elevation neighbour. This geometry then remained fixed for the remainder of the debris slide’s travel.

Given Vinit, slide depth, width, length of the grid cell to grid cell hypotenuse, and the grid cell to grid cell slope angle, the model then simulated entrainment and deposition of slide material using the series of volumetric regression equations described in Wise (1997). One complication was the inability to calculate bend angle (Wise 1997) in the simulations because the path azimuth could not be determined using the map information available during prototype development. This introduced some unaccounted uncertainty as to the accuracy of the regression equations for deposition, which included bend angle as an independent variable. It was recognized that excluding bend angle and re-running the regression analyses would be the most efficient solution (Jonathan Fannin, UBC Civil Engineering, *pers. comm.* 1998). In the test application of FFIP-MM, the interim solution was to fix bend angle to its average surveyed value (5.2). In any case, bend angle did not appear to be a very important explanatory variable for predicting slide volume and travel distance on the 449 slides surveyed on the Queen Charlotte Islands.

Slides initiating in or entering gullies were assumed to entrain sediment (not LWD) based on a fixed gully debris yield rate (10 m^3 sediment per m gully) because the required map information was not available at a fine enough scale. As a result, it was not possible to obtain adequate estimates for the values of the predictor variables for the confined flow regression equations in Wise (1997). For gullies, once a failure occurred, the gully recharged at a constant annual rate (12.5%) until fully charged 8 years later.

As the slide moved downslope, it differentially entrained volumes of standing (rooted) and downed (unrooted) LWD along the debris path. The proportion of standing and downed LWD entrained was assumed to depend on the incoming volume of the slide (Tables A10 and A11, Appendix A). The initial debris composition was assumed to include coarse sediment, fine sediment, this new LWD, and fine organic debris. When a debris slide entered a stream reach, the volume of coarse sediment and LWD were added to the stream reach (fine sediment and organics were assumed to be flushed through high-energy coastal watersheds on the annual time step used in the simulations).

2.2.5 Channel submodel

This component of the model converts the effects of changes in the watershed to changes in reach CAP states. The objective of the submodel is not to accurately predict sediment and LWD movement, but to provide qualitatively reasonable rates of movement, and changes in CAP style. Under CAP, measurements of channel slope, width, depth, and tractive force are used to classify the channel into one

of seven morphological types (e.g., Riffle-Pool), and one of seven disturbance levels or states (e.g., D3 = severely degraded, S = stable A3 = severely aggraded); (see BC Ministry of Environment 1996). For the test application of FFIP-MM, Carnation Creek was divided into 47 reaches of known CAP morphology ranging from approximately 100m to 1km in length (Figure 3). The channel submodel relied on a mass balance approach to represent coarse sediment and LWD volumes present within the individual reaches. No attempt was made to track the locations of LWD (e.g., log jams) within each reach. A generalized flow-chart of the submodel (Figure 4) indicates its major components.

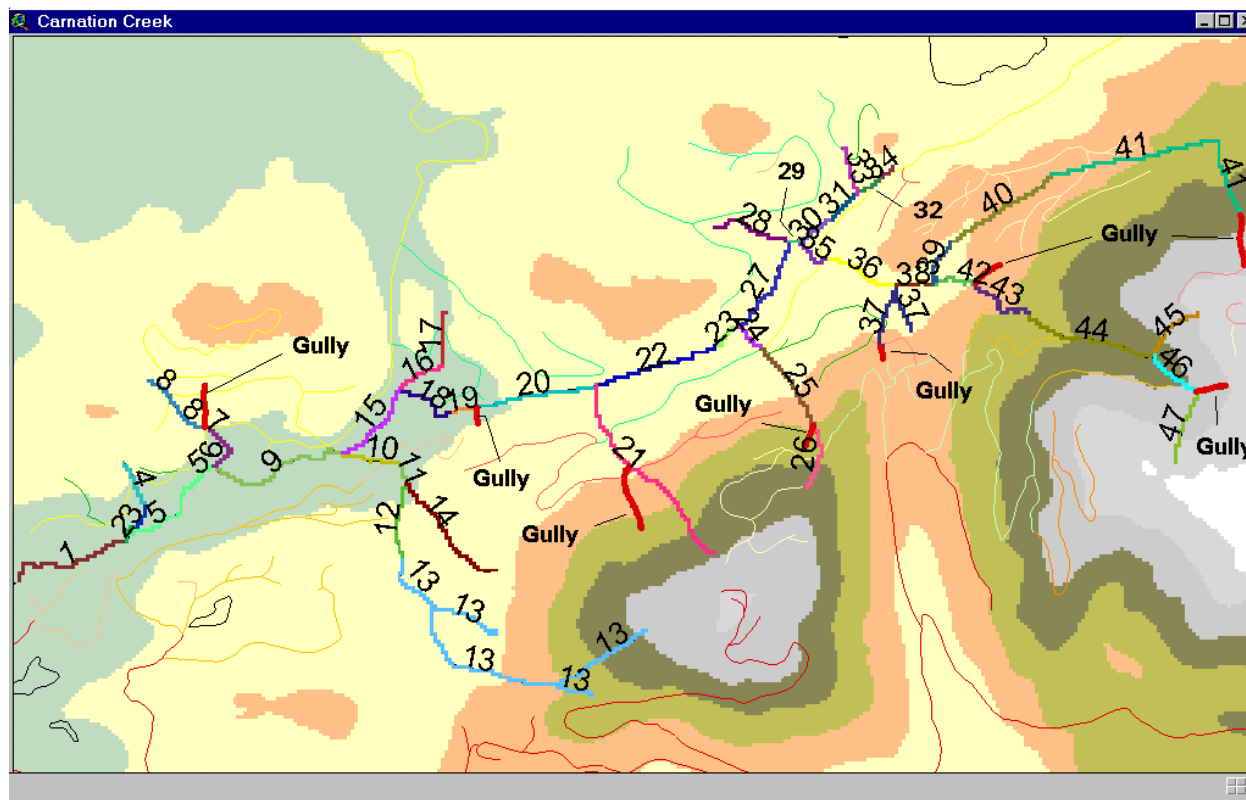


Figure 3: Reaches used in the test application of FFIP-MM to Carnation Creek. Colors for individual reaches are used for contrast. The thick red lines are gullies. The general relief for Carnation Creek is indicated.

Using the input volumes of sediment and LWD from the upslope submodel, the channel submodel converted the sediment storage volume for each reach to a reach specific CAP state. In brief, LWD obtained from upstream reaches, riparian areas, and debris slides were added to the current reach. κ (equation 1) was then applied to decay this volume of LWD. Next, a log-normal random variable with a mean of 1 and a SD of 0.1 was used to simulate annual variation in the downstream movement of LWD resulting from storm flow events. The movement rate was determined by applying the log-normal random variable to the equilibrium LWD loss rate determined during the calibration step ($FL_{e,r}$ equation 1). Because sediment storage is known to be directly related to LWD volumes (Bison *et al.* 1987 as cited in Hartman *et al.* 1996), the current proportion of a reach's volume storing LWD was used to determine a "sediment capacity" (Γ equation 2) for the reach (Table A4, Appendix A). The sediment capacity volume was used to quantify the volume of sediment that would be protected by the LWD, and therefore immune to flushing by storm flows (Figure 3). Sediment volumes exceeding the sediment capacity volume were, like LWD, subject to downstream movement. The volume of sediment moving downstream was

determined by applying a log-normal random variable with a mean of 1 and a SD of 0.25 to the equilibrium sediment loss rate determined during the calibration step (FS_{er} equation 2). Again, the use of a stochastic flushing rate for sediment, like LWD, was used to account for interannual variation in peak flow intensity. Years with high intensity storms have both more landslides (higher probability of slope failure), and more in-channel movement of LWD and sediment.

Once the FL and FS values are applied and LWD and sediment storage volumes were updated, the current proportion of the reach's volume storing sediment was used to determine its CAP state. This was achieved using Table A3 (Appendix A). Given a reach's CAP morphology, and the proportion of its volume filled with sediment, the values in Table A3 determine the reach's CAP state.

Further amounts of sediment can be recruited from a reach's banks when it is aggrading (e.g., $S \rightarrow A1$) because stream-flow is often directed at the banks of the reach in the aggraded state (Mike Church, University of British Columbia, Department of Geography, *pers. comm.*, 1997). This sediment input source was taken into account by applying the multipliers found in Table A12 (Appendix A) to the net annual increase in sediment storage.

It is important to point out that the use of a log-normal distribution to represent variation in movement rates of LWD and sediment was arbitrary, and in future, should be based on expert judgement. It was pointed out that a gamma distribution may be a more appropriate distribution to represent variation in LWD and bedload sediment movement rates (Mike Church, University of British Columbia, Department of Geography, *pers. comm.* 1997).

2.2.6 Habitat capability submodel

An expert elicitation was held November 5th and 6th 1997 with eight fish habitat biologists to obtain relative habitat capability values (on 1 to 5 scale) for the 49 CAP type and state combinations. Photographs of examples of stream reaches with different CAP types and states were used, together with descriptions from the CAP Guidebook to provide participants with both visual and descriptive information when making their independent evaluations. Evaluations were completed for three species: coho salmon, pink salmon, and steelhead. For pink salmon, it was felt that the spawning and incubation habitat was likely to be the most limiting to smolt production overall. Therefore, participants rated only this type of habitat for each of the CAP types and states. For coho salmon, three different types of habitat were considered: 1) spawning and incubation; 2) summer rearing; and 3) overwintering habitat. In addition, participants provided an “overall rating”, which assumed that coho were spatially restricted to the CAP type indicated. For steelhead, it was decided to rate the different CAP types and states in terms of life-stage specific survival rates. That is, the 1 to 5 scale represented the relative survival associated with different habitat types and states. The three life stages selected were: 1) egg to fry survival; 2) fry to parr survival; and 3) parr to smolt survival. Again, participants provided an “overall rating” by assuming that steelhead were spatially restricted to the CAP type indicated.

The group recognized that there are many factors that influence fish density and survival other than CAP type and state. These include: hydrology, temperature, nutrients, habitat complexity, food abundance, interspecific interactions, and the accessibility of habitat within the watershed. It was felt that the best way to handle some of these other factors was to consider them incrementally as additional modifiers to the habitat ratings derived purely from CAP type and state in future versions of FFIP-MM. Currently, the prototype model generates probability distributions for the following length weighted watershed habitat capability rating:

$$\overline{WHC}_{species,life-stage} = \sum_{r=1}^{47} \left[\left(\frac{L_r}{\sum_{r=1}^{47} L_r} \right) \times \overline{HC}_{CAPtype, CAPstate, species, life-stage} \right] \times 20 \times \vartheta$$

... [3]

where:

$\overline{WHC}_{species,life-stage}$ is the watershed wide habitat capability rating on a 0 to 100 scale for a particular species and life-stage,

L_r is the length of reach r ,

\overline{HC} is the mean habitat capability rating from the eight fisheries biologists for the CAP type, state, species and life-stage in question, and

ϑ is a scaling factor obtained by dividing 100 by the result of equation 3 for the watershed in its assumed pristine condition – without the ϑ term. That is, a length rather than area weighted scheme was used for the WHC rating because the CAP morphology assignment already accounts for stream width, and the habitat biologists considered this in their ratings.

Since the model explicitly incorporates natural variation in several components, the ultimate output of FFIP-MM are probability distributions of WHC for alternative harvesting strategies over time. Less spatially aggregated output is also available, such as the species and life-stage specific ratings for

individual reaches. This report presents the life-stage specific results for coho salmon. The \overline{HC} values for coho spawning and incubation, overwintering, and rearing are provided in Figure 5.

Other FFIP researchers are currently developing empirical relationships between adult escapement and smolt production estimates and CAP. The results from this research can be easily incorporated into FFIP-MM, (i.e., supplement expert opinion WHC values with an empirical smolt capacity index).

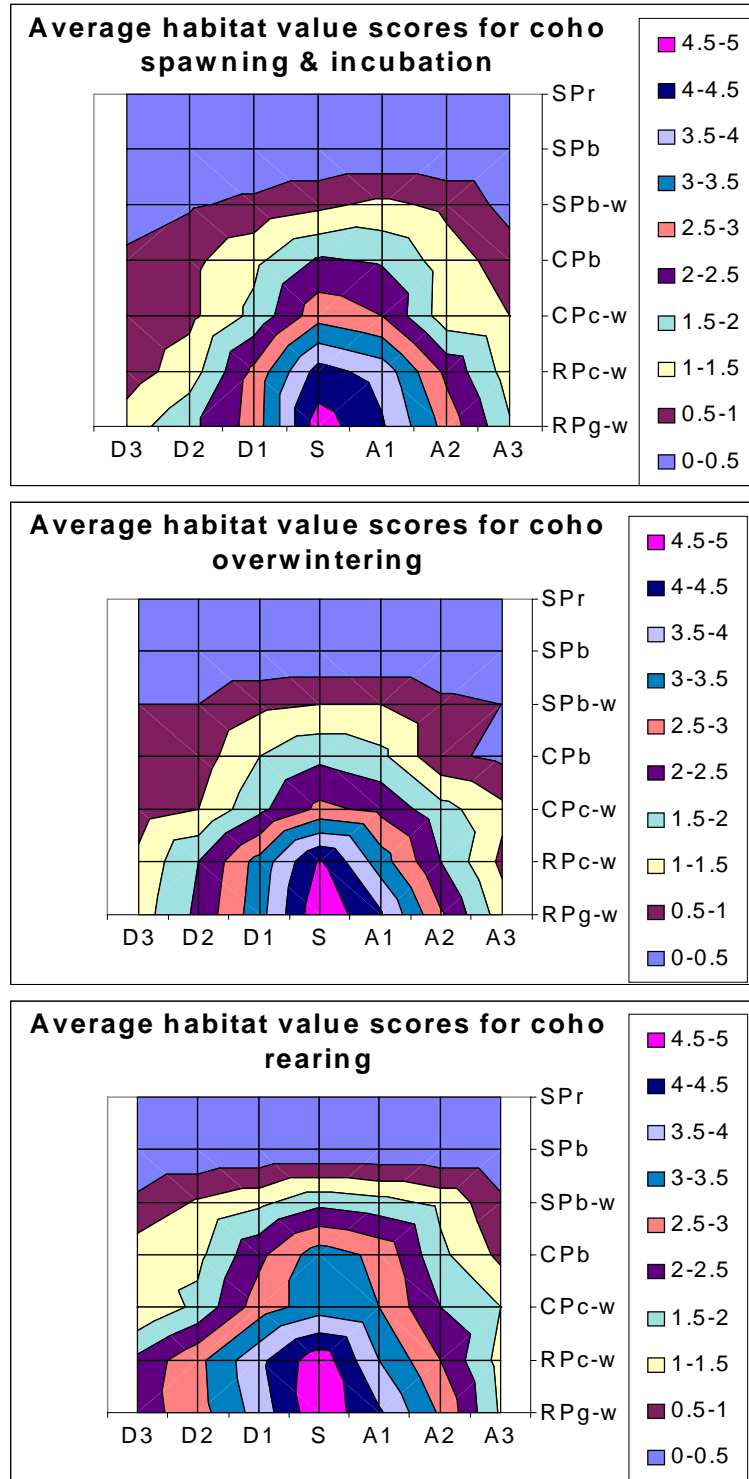


Figure 5: Results of an expert elicitation of the habitat capability value of different CAP type and states for coho salmon.

3.0 Preliminary Results and Discussion

Many of the parameter values for Upslope and Channel submodels were assigned with minimal input from the FFIP-MM research group, though the functional forms were developed through group discussions. Future work will be required to refine model parameters and expert rules and to define alternative management scenarios before the model is rigorously applied to a particular watershed. By examining model behaviour in relation to historical impacts of logging in Carnation Creek (as described in Hartman *et al.* 1996) for this *preliminary* set of rules and parameters, this report serves as the first step in model evaluation. Further model evaluation will require ongoing participation by the FFIP-MM research group.

This section also provides model results under an unlogged, pristine condition to ensure internal consistency (e.g. watershed CAP states should stabilize and do not continuously degrade or aggrade over time).

3.1 Calibration

Figure 6 shows the simulated frequency of stream impacting slides in different regions of Carnation Creek in the pristine condition. The average volumes of sediment and LWD inputs obtained in this manner provided the raw inputs necessary to determine the steady state values for $FL_{e,r}$ (equation 1) and $FS_{e,r}$ (equation 2); (Figure 7).

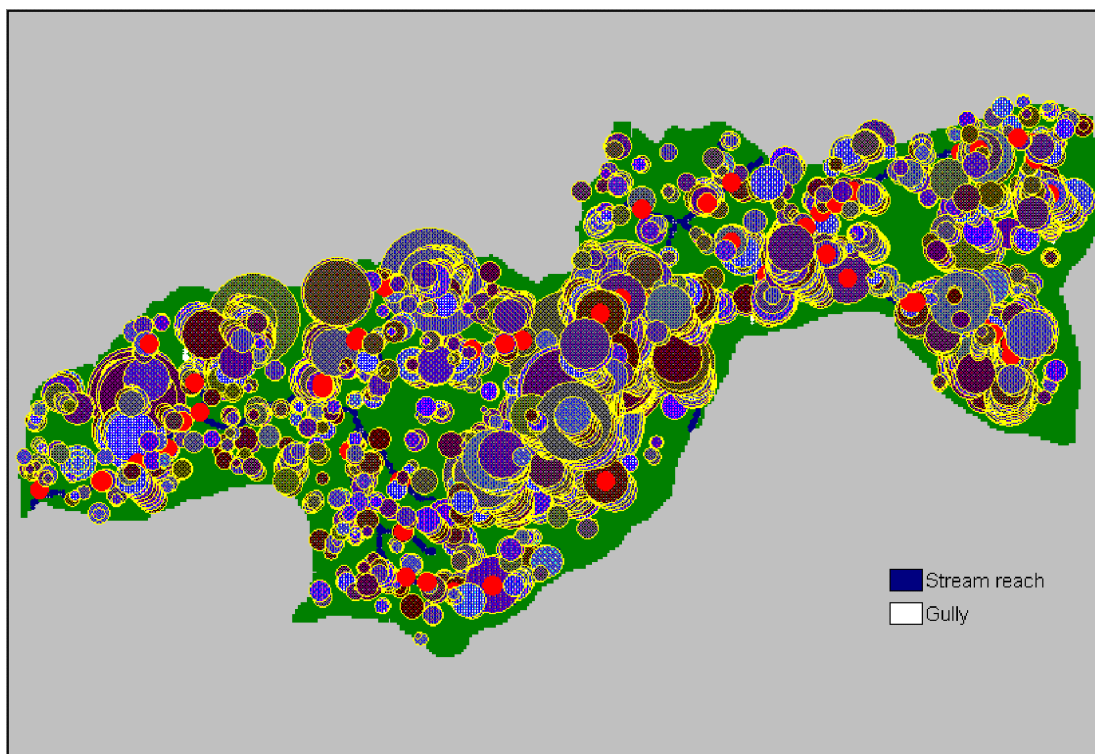


Figure 6: Debris slide history for a 1000 year simulation of Carnation Creek in the ‘pristine’ condition. Red circles indicate stream impacting debris slides. The blue shaded circles indicate the debris slide paths and *relative* magnitudes for the individual events.

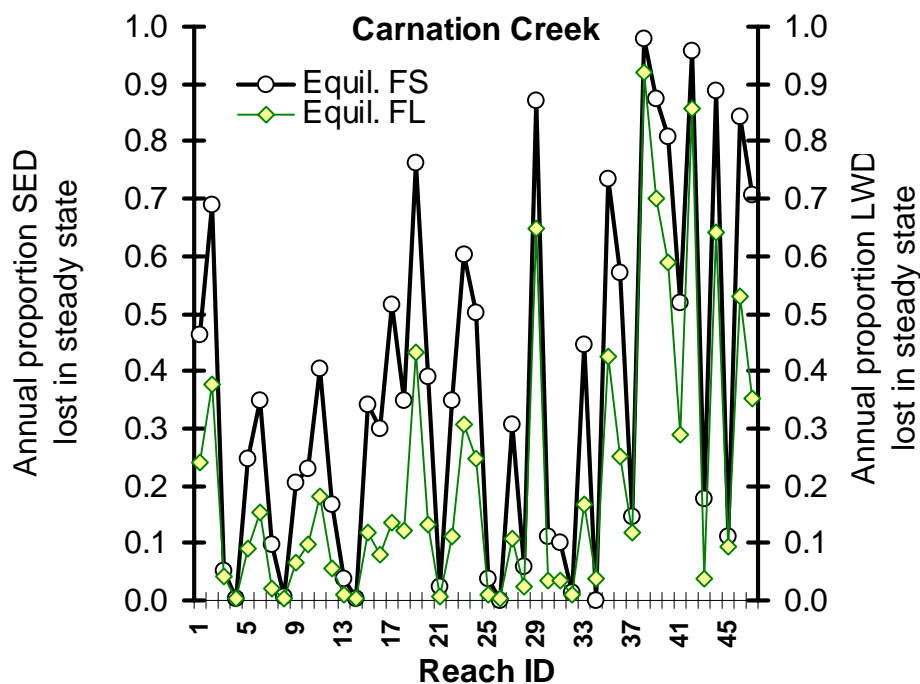


Figure 7: Calibration results.

An extremely wide range of variability was observed in the steady state movement rates for both sediment (0 to 0.98) and LWD (0.0021 to 0.92) among reaches. The rate of LWD movement was generally lower than the sediment movement rate. Reaches 38, 42, 44, 29, 39, 46, 35, 47, 40, 19, 23, 36, and 17 (Figure 3) all gave annual sediment bedload movement rates greater than 50% (Figure 7). The pattern of stream impacting slides in Figure 6 shows that a higher frequency of landslide inputs is predicted for these reaches (refer to Figure 3 for the locations of the individual reaches). Therefore, greater movement rates would be required to maintain the pristine CAP state. The realism of these steady state values needs to be assessed. If the landslide and gully input rates are realistic but the sediment and LWD movement rates are too high, the way in which the steady state movement rates are used in the simulations needs to be re-evaluated (e.g. consider using a finer time-step, or a means of using the steady state movement rates to parameterize reach specific probability distributions for movement, etc.).

Unrealistically large steady state movement rates for sediment and LWD are also of concern because these rates are currently multiplied by log-normal random variables to represent variation in peak storm flows, and therefore, flushing rates. When a reach's sediment or LWD movement rate exceeds 0.5 per year, application of the log-normal deviate can result in the movement rate being truncated at 1. As such, if the steady state movement rates are realistic, the use of log-normal probability distribution may not be appropriate. The FFIP-MM research group should address this issue by considering the likelihood of 100% of the material in a particular reach being flushed downstream within a single year.

For headwater reaches 26 and 34 (Figure 3), the annual sediment movement rate was 0. This occurs when the upslope submodel predicts that the reach in question will never receive any input from upstream reaches or via landslide material. One or more of three possible mechanisms explains this result. First, landslide inputs of sediment to a reach could be zero if there was a formulation or parameterization error

in one or more of the volumetric regression equations. Alternatively, if the upslope terrain around these reaches is inherently stable or low gradient, then landslide inputs may rightly be nil. Thirdly, spatial approximation error in one or more map layers could also produce this result (e.g. spatial interpolation error in the grid cell elevation values, the use of grid cells that are too large, or incorrectly mapping the position for the stream reach). The likelihood of not obtaining any inputs of sediment from landslides to a given reach will also increase as the length of the reach decreases (and vice versa). Headwater reaches will naturally experience a lower rate of sediment input because landslide inputs are their only sediment source in the simulations. Reaches receiving no inputs of sediment from landslides will maintain their initial CAP state assignment for the duration of any simulation.

3.2 Upslope submodel

The mean number of stream impacting landslides peaked first in 1980 and again in 1991 for the historical logging scenario (Figure 8). The peak number of stream impacting landslides from roads lagged behind, with the first peak occurring in 1991 then again in 1995 (Figure 8). The peaks in number of stream impacting landslides corresponded with the two major phases of clear-cut logging: during 1976 to 1981, 41% of the watershed was clear-cut, then between 1987 to 1994, another 42% was harvested (Hartman *et al.* 1996). Simulated landslide frequencies remained elevated between 1975 to 2020 before returning to their simulated pre-logging frequencies (Figure 8). The increase in the simulated mean number of stream impacting slides was due to the introduction of logging roads and clear-cuts which increased the probability of slope failure (Figure 9). Figures 10a and 10b show the roading and logging patterns in 1980 and 1991.

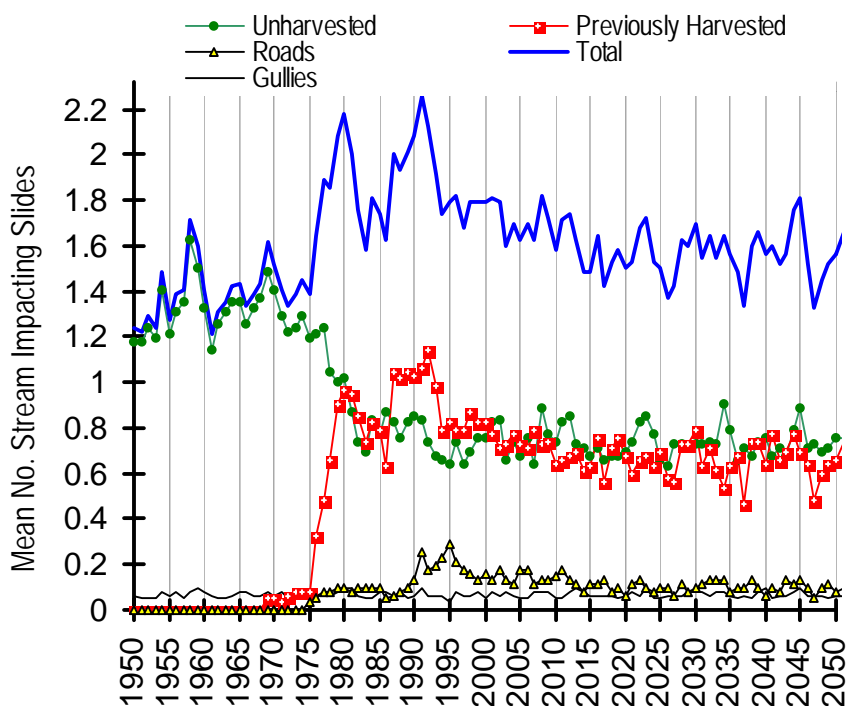


Figure 8: Simulated mean number of stream impacting slides between 1950 to 2100 (averages over 70 Monte Carlo trials).

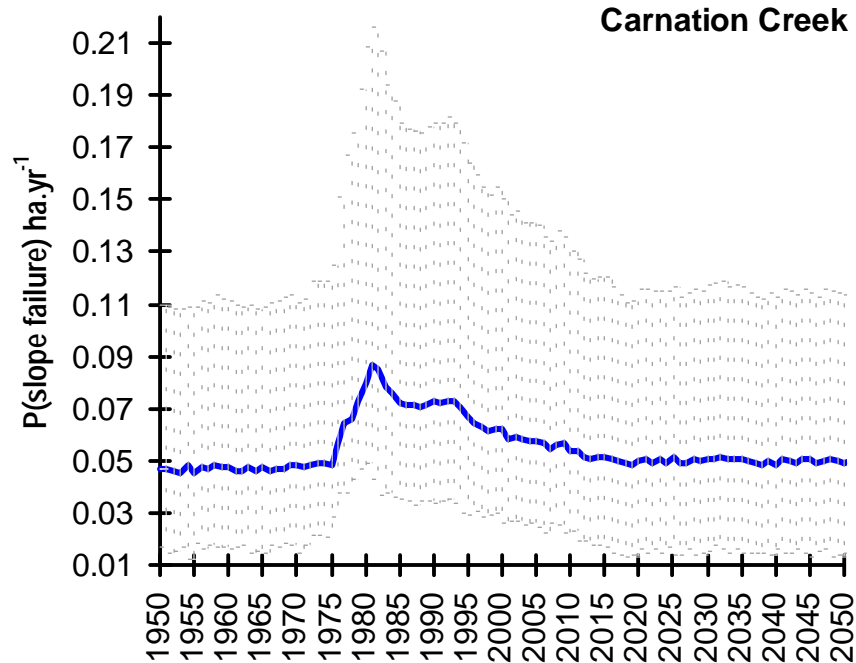


Figure 9: Simulated mean probability of slope failure between 1950 to 2100 (averages over 70 Monte Carlo trials), +/- 1 SE.

While the trends in Figure 8 seem reasonable, the simulated mean number of stream impacting slides need to be compared with the available empirical data and expert judgement. Specifically, was the simulated increase as large as that observed or expected? In addition, the number of stream impacting slides arising from old growth terrain, clear-cuts, roads, and gullies must be compared with said data and expert judgement. For example, clear-cut related landslides contributed to a significantly larger number of stream impacting slides between 1987 to 1994 (second phase of clear-cut logging) and not during the first phase (1976 to 1981). Is this realistic? Also, in the context of the spatial pattern of harvesting in Carnation Creek, is it reasonable that approximately the same number of stream impacting slides arise from old-growth and clear-cut terrain (Figures 8, 10a, and 10b)? If the answer is no then the difference in the probability of slope failure between old growth and clear-cut terrain is either not large enough, or there is a parameterization or formulation problem with one or more of the volumetric regression equations. A larger issue related to the use of the volumetric regression equations is the validity of applying the volumetric regression equations to old growth terrain when it is known that these equations were parameterized using data for 6 to 15 year old clear cuts on the Queen Charlotte Islands. The likely first step to improving the predictive accuracy of the volumetric regression equations is to remove unnecessary or unavailable predictor variables (namely the bend angle variable). While this may increase variability in debris travel distances and volumes, gains in accuracy will likely occur.

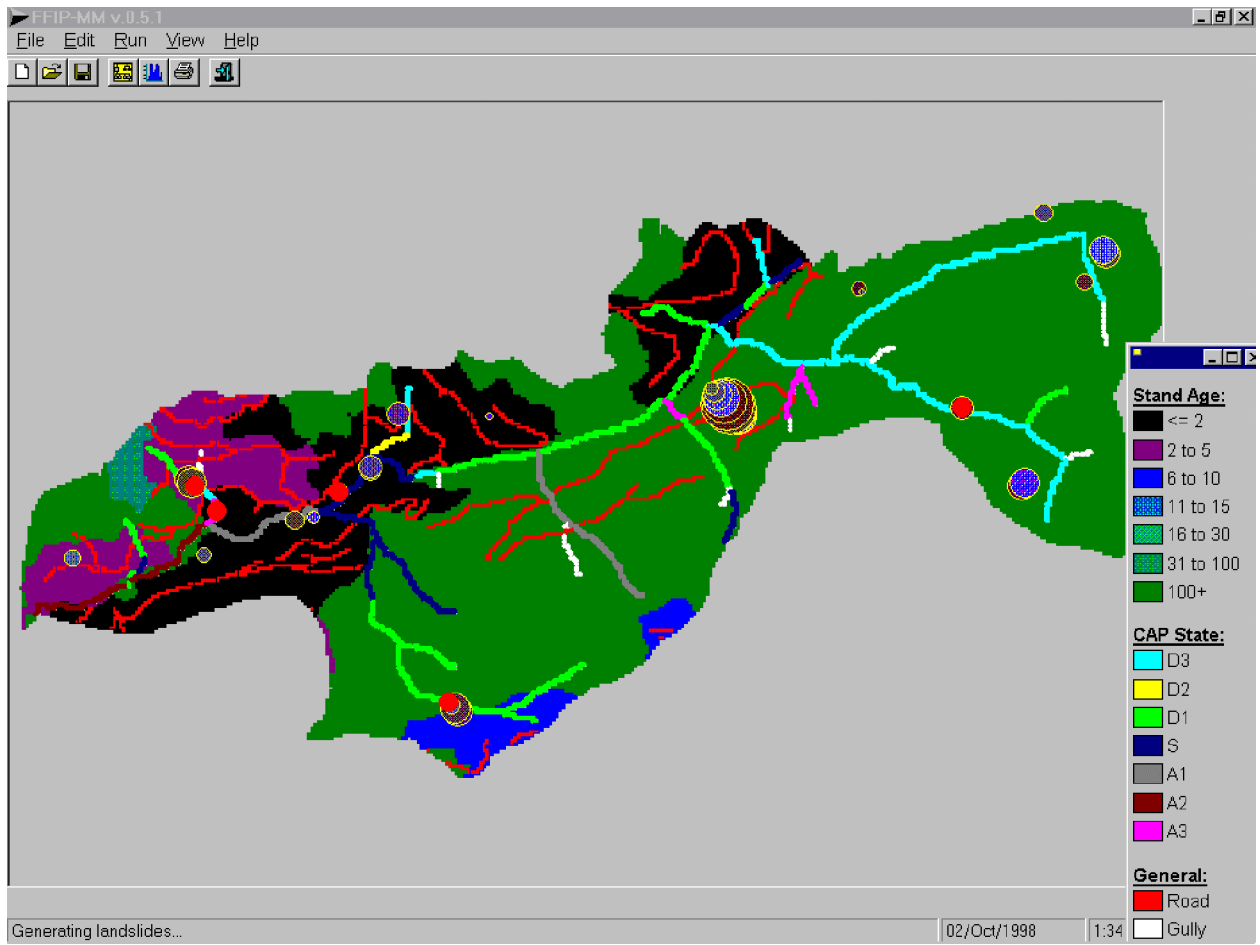


Figure 10a: Road and cut block locations (forest age structure) in 1980.

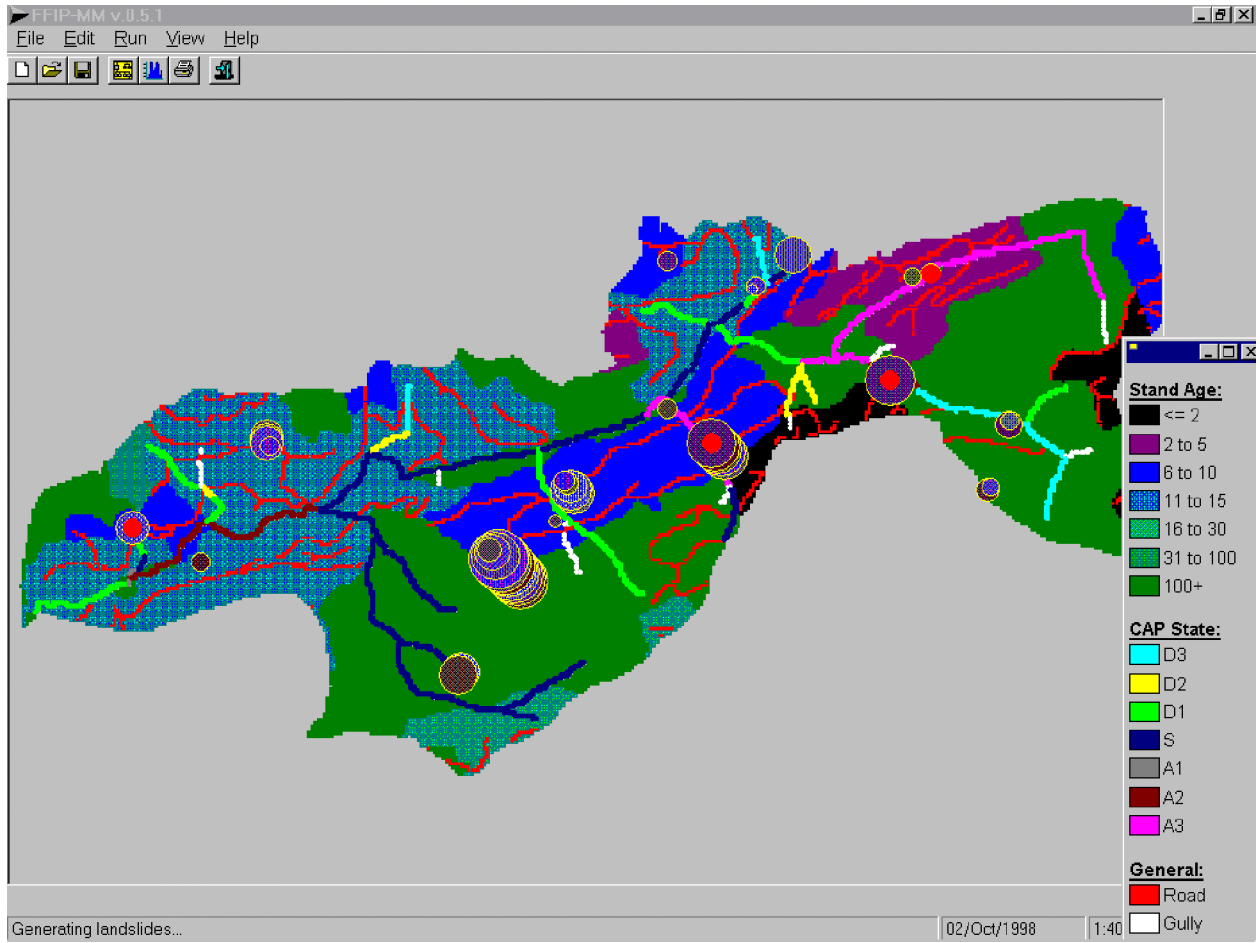


Figure 10b: Road and cut block locations (forest age structure) in 1991.

3.3 Channel submodel

3.3.1 Watershed Wide Results

The simulated watershed wide storage of sediment decreased early on during the first phase of logging then increased steadily until 1994 (end of the second major phase of logging) before decreasing towards the simulated pristine storage volume (Figure 11). Simulated LWD storage volumes remained relatively constant during the first phase of logging, but after 1980 began to decline (Figure 11). Unlike sediment storage, simulated LWD storage volumes did not recover to their pre-logging volumes by 2100 (~100 years after logging). This result is consistent with previous LWD research that suggests LWD volumes can take upwards of 300 years to recover when riparian stands are harvested (Hartman *et al.* 1996, McHenry *et al.* 1998). Because sediment accumulates behind LWD, it is reasonable to expect that the reduction in LWD storage volumes would correspond with a reduction in sediment storage. This was true between 1974 and 1980 after which simulated sediment storage volumes increased steadily until 1994, until they again tracked the reduction in LWD volumes (Figure 11). This suggests that the loss of LWD in certain reaches had a disproportionate effect on sediment storage volumes between 1974 and 1980, but that when logging was the most intense (~ 1980 to 1994), sediment input from landslides overwhelmed the sediment losses attributable to reduced LWD volumes.

While the trends in watershed wide LWD and sediment storage volumes appear to make sense, the magnitude of the changes was less than expected. Average simulated sediment storage volumes varied by only 6000m³ (over ~ 156,000m³ stream network) following logging. Hartman *et al.* (1996) noted that logging between 1976 to 1994 caused deposition of ~ 25, 480m³ of sediment. However, the simulated cumulative sediment deposition over this period was just 7, 944m³ (31% of the observed deposition). Several factors could explain this difference: (1) sediment input volumes from landslides may be smaller than observed, (2) Average LWD and/or sediment movement rates were too high, (3) the simulated volume of sediment stored by LWD was too low, and/or (4) LWD storage volumes were too high, thereby “squeezing” out sediment. Most likely, a combination of these factors produced the difference in observed and simulated sediment storage volumes.

Average simulated LWD storage volumes were three times those observed in logged streams throughout the Pacific Northwest (Figure 12). This suggests that the model was calibrated with too much LWD and/or inputs of LWD from riparian tree fall and/or debris slides were too great. However, the rate of decline in LWD following logging closely matched the observed post-logging rate of decline in LWD (Figure 12).

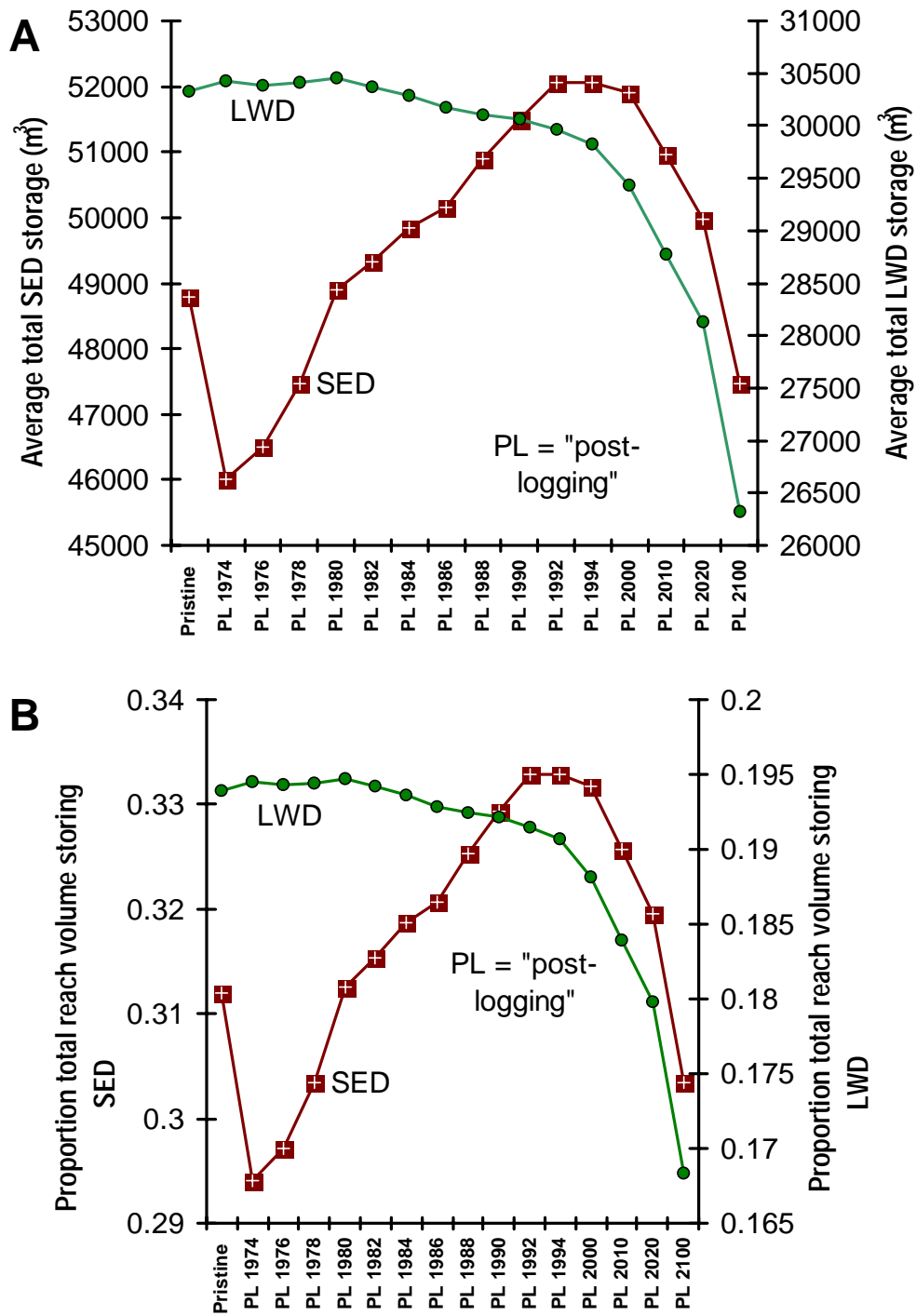


Figure 11: Simulated watershed wide trends in sediment and LWD storage volumes. Note the change in scale after 1994.

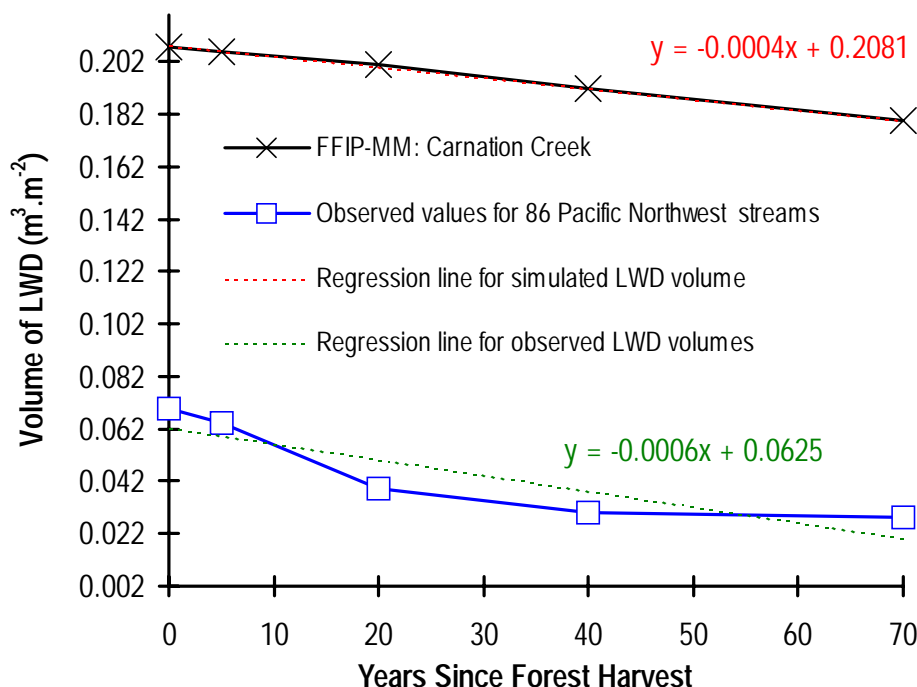


Figure 12: Average watershed wide volume of LWD simulated by FFIP-MM (for 70 Monte Carlo trials) in comparison with the observed mean volumes of LWD for 86 streams surveyed throughout the Pacific Northwest (data from Hartman *et al.* 1996).

3.3.2 Results for Select Reaches

Figure 13 provides the simulated average inputs of sediment from landslides in select reaches in the lower main channel, canyon, and upper tributary areas of Carnation Creek. For the selected reaches, inputs of sediment from landslides were only significantly larger in the mainstem area between approximately 1980 and 1990 (Figure 13A). A similar pattern was observed for LWD inputs from landslides (Figure 14). Figure 15 shows the reduction in riparian input of LWD to several select reaches associated with logging to the stream banks. The volumes of sediment and LWD input from landslides need to be compared with the available empirical data and expert judgement. Likewise, we need to assess the veracity of the LWD input volumes from the riparian area.

The effects of logging in Carnation Creek on total sediment and LWD storage volumes are given in Figures 16 and 17 respectively, for selected reaches. Again, the volume of sediment and LWD stored in the tributaries in the upper watershed were least altered by forestry activities, while the lower mainstem reaches were the most significantly altered. This is consistent with the general trends reported in Hartman *et al.* (1996). It should be pointed out that the initial decrease in sediment storage volumes between 1960 to 1970 was largely due to the model progressing away from its initial conditions towards the pristine state (Figure 18). Nevertheless, after 1970 when logging began in the lower value of Carnation Creek (including the upslope areas adjacent reach 5) simulated sediment storage initially declined further than that which occurred in the pristine condition (Figure 18). Presumably, this was due to the reduction of LWD inputs and storage volume. However, starting in 1980 sediment storage volume in the lower mainstem steadily increased until 2005. Thus, simulation results suggest that the increased rate of landslides and resultant sediment inputs overwhelmed the decline in sediment storage due to LWD.

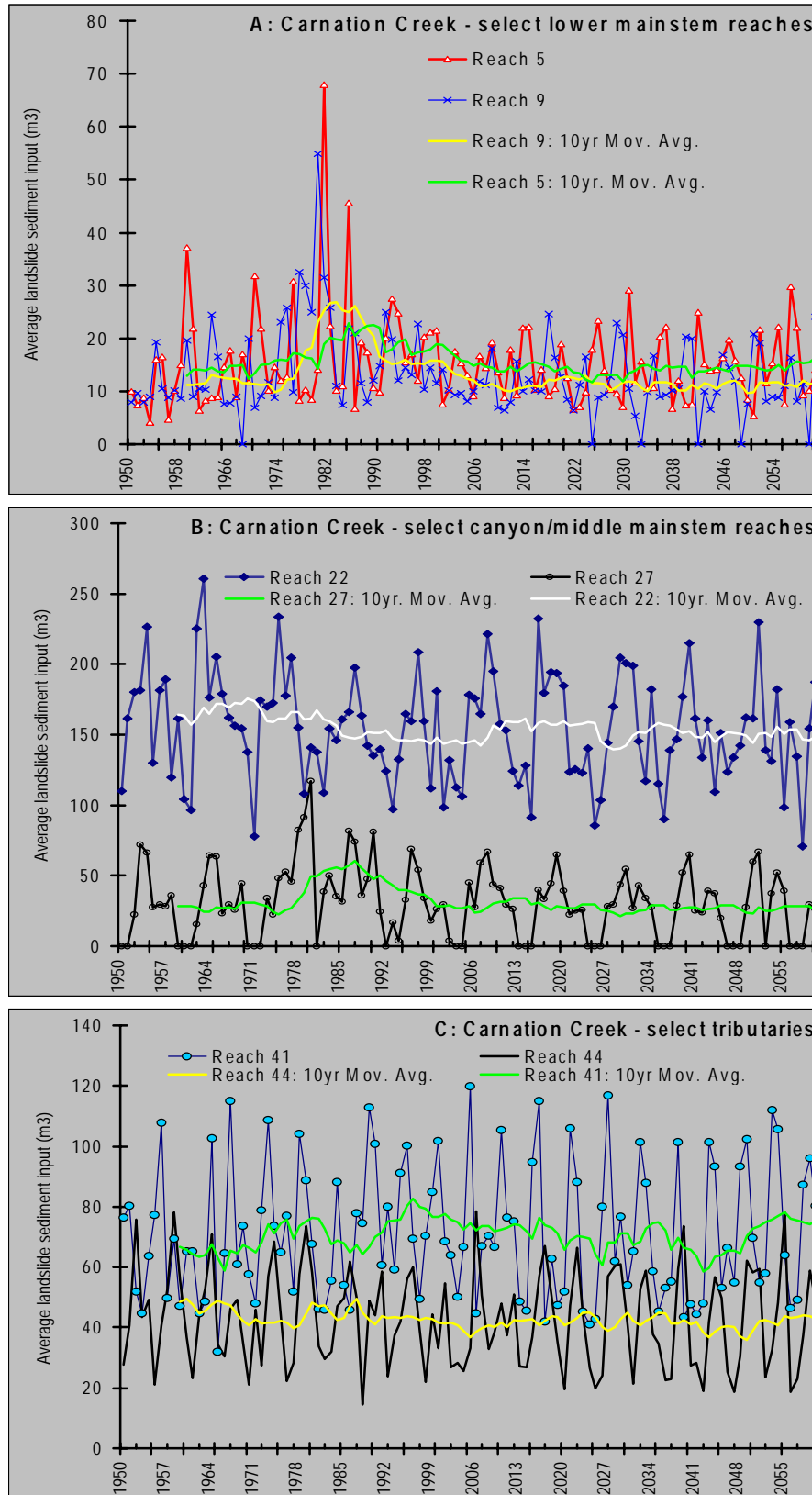


Figure 13: Simulated average annual landslide inputs of sediment from 1950 to 2060 in three different regions of Carnation Creek.

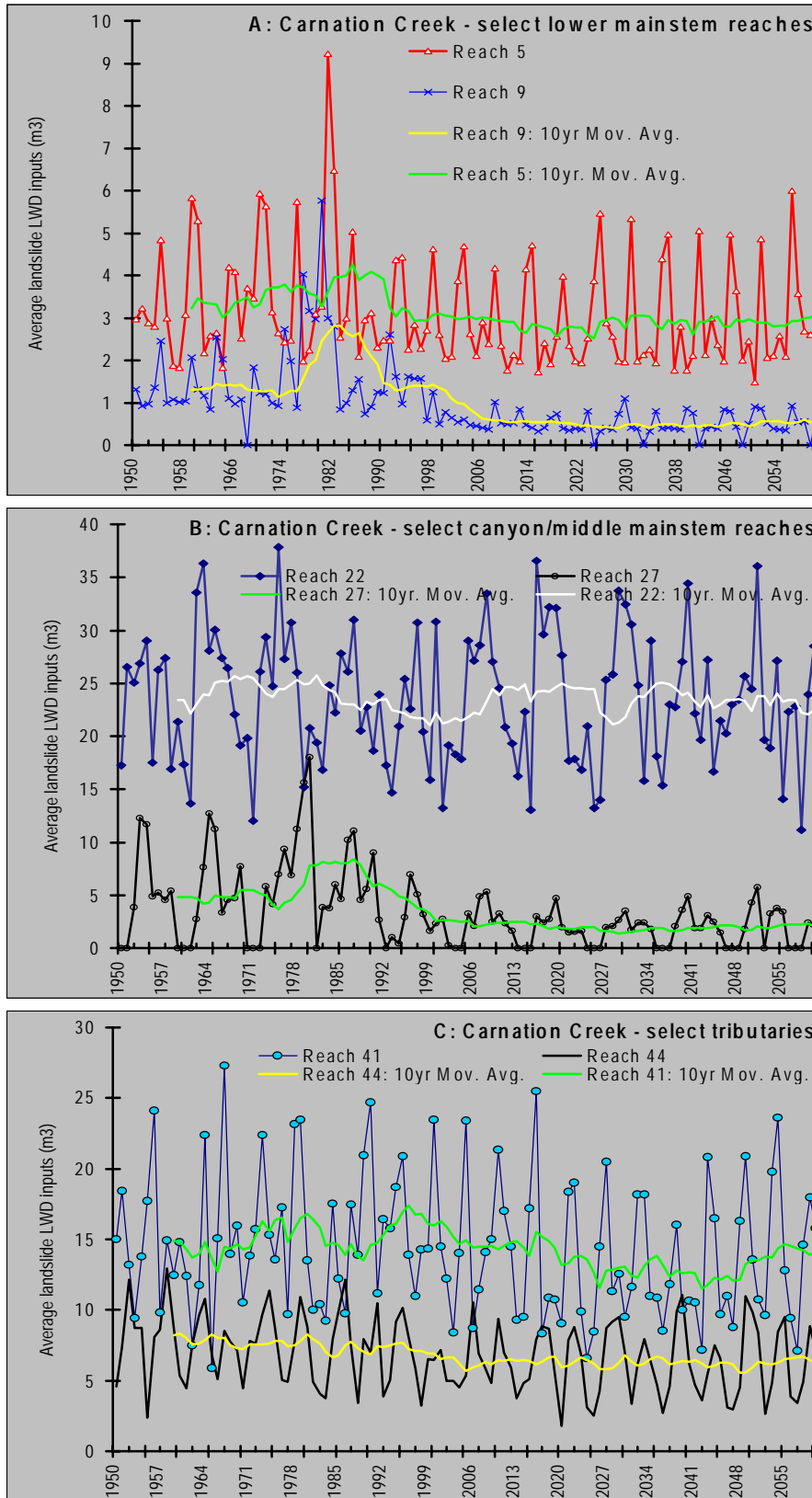


Figure 14: Simulated average annual landslide inputs of LWD from 1950 to 2060 in three different regions of Carnation Creek.

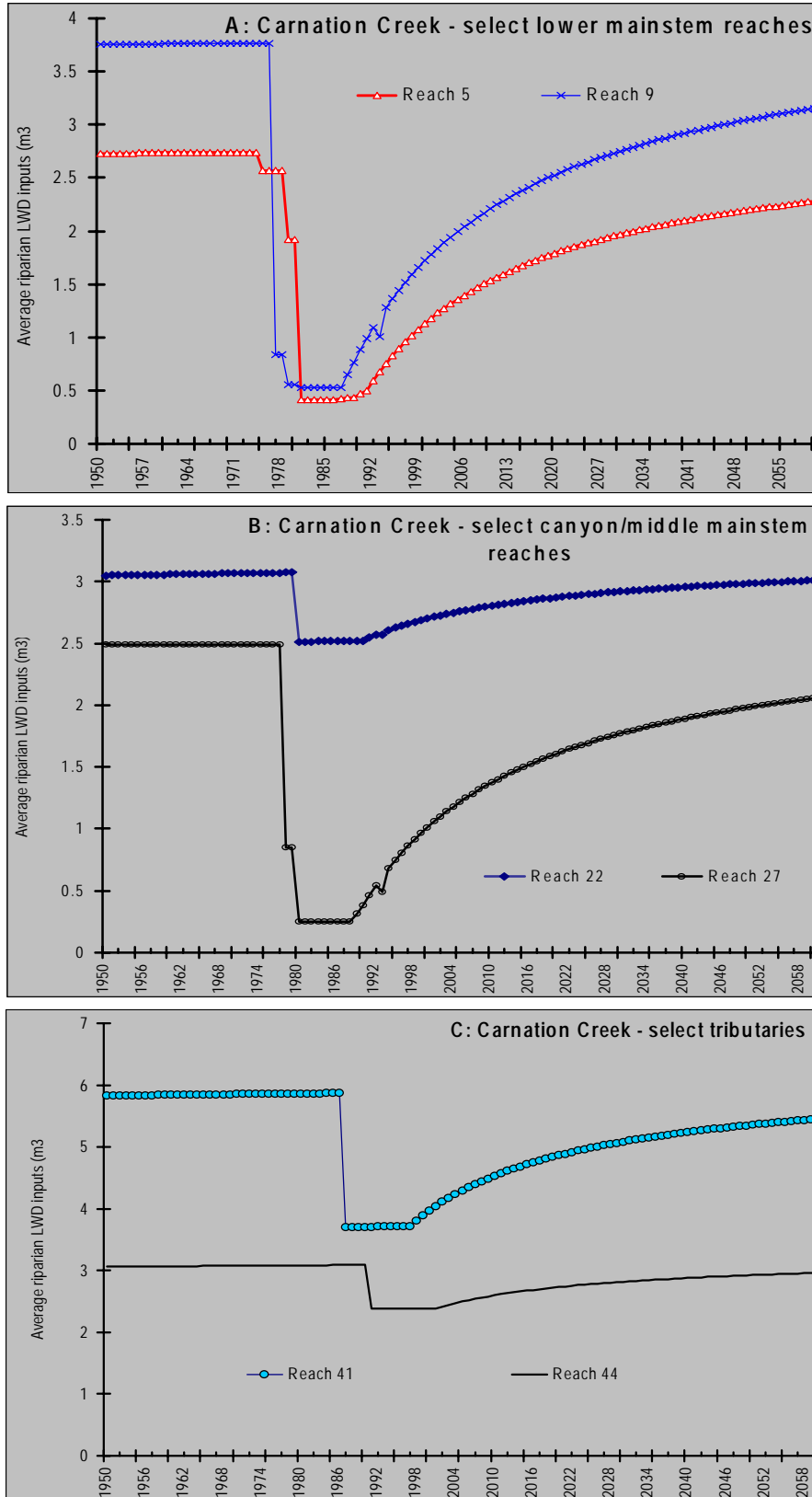


Figure 15: Simulated average annual riparian inputs of LWD from 1950 to 2060 in three different regions of Carnation Creek.

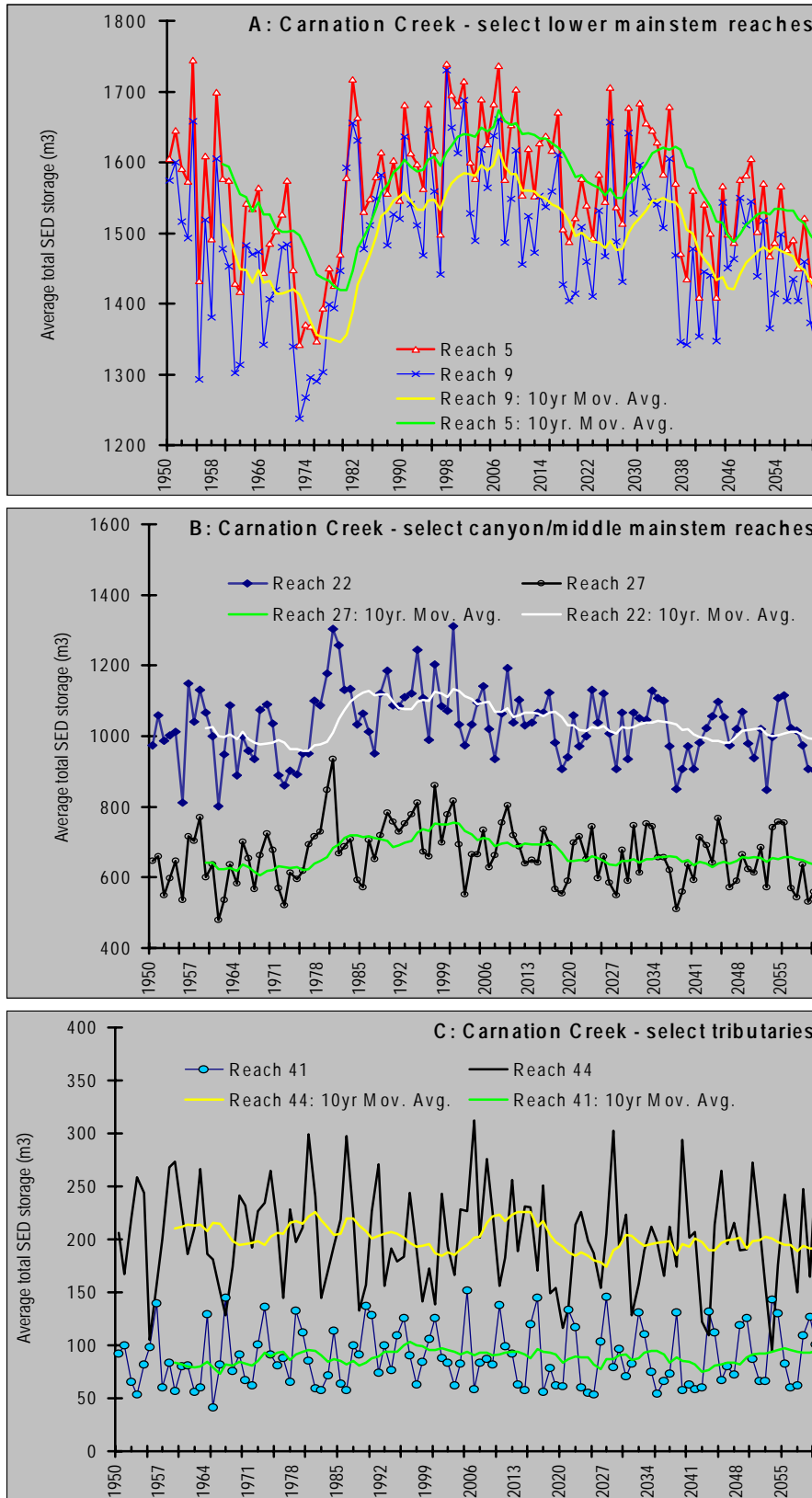


Figure 16: Simulated average sediment storage volumes from 1950 to 2060 in three different regions of Carnation Creek.

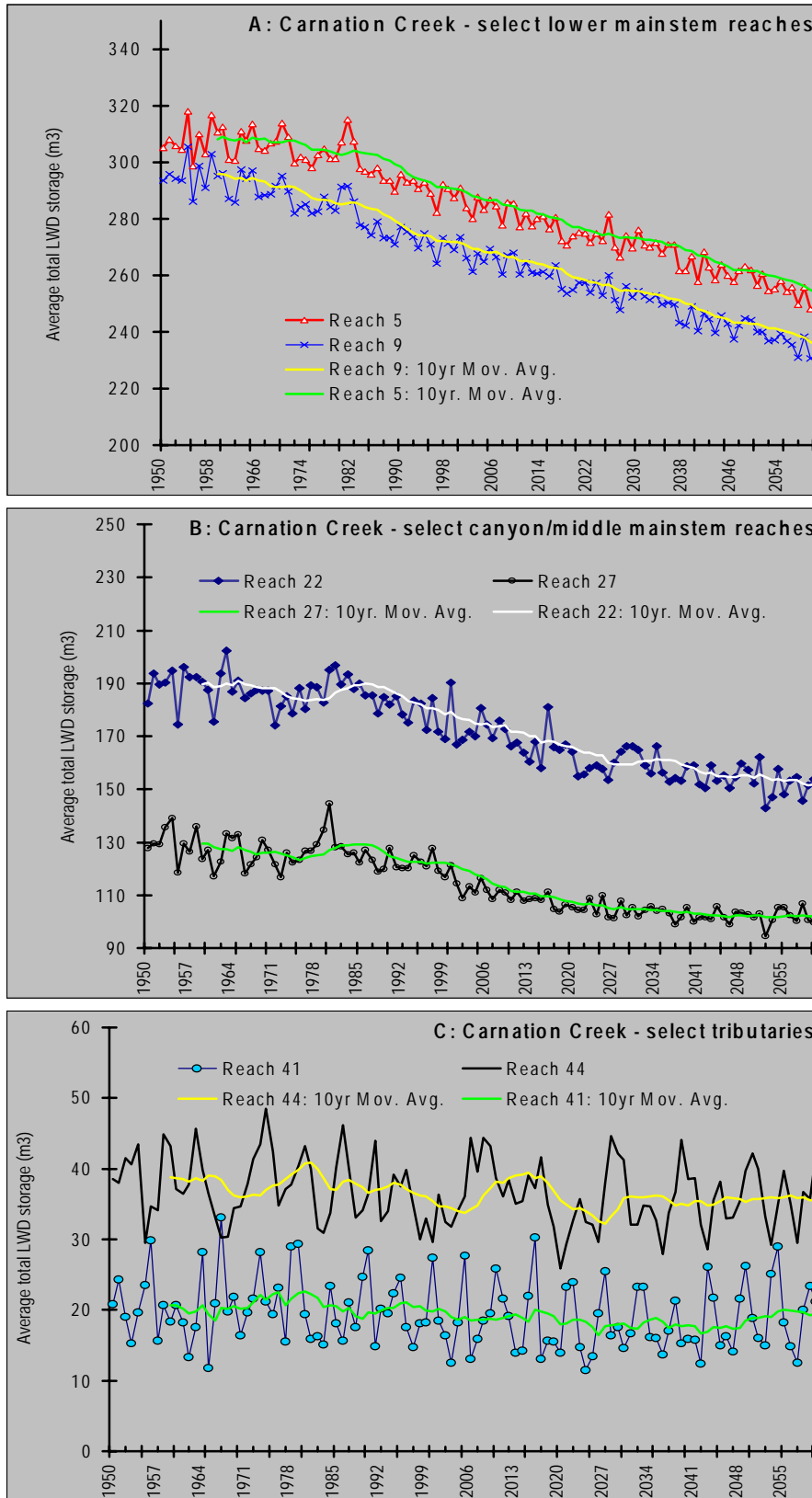


Figure 17: Simulated average LWD storage volumes from 1950 to 2060 in three different regions of Carnation Creek.

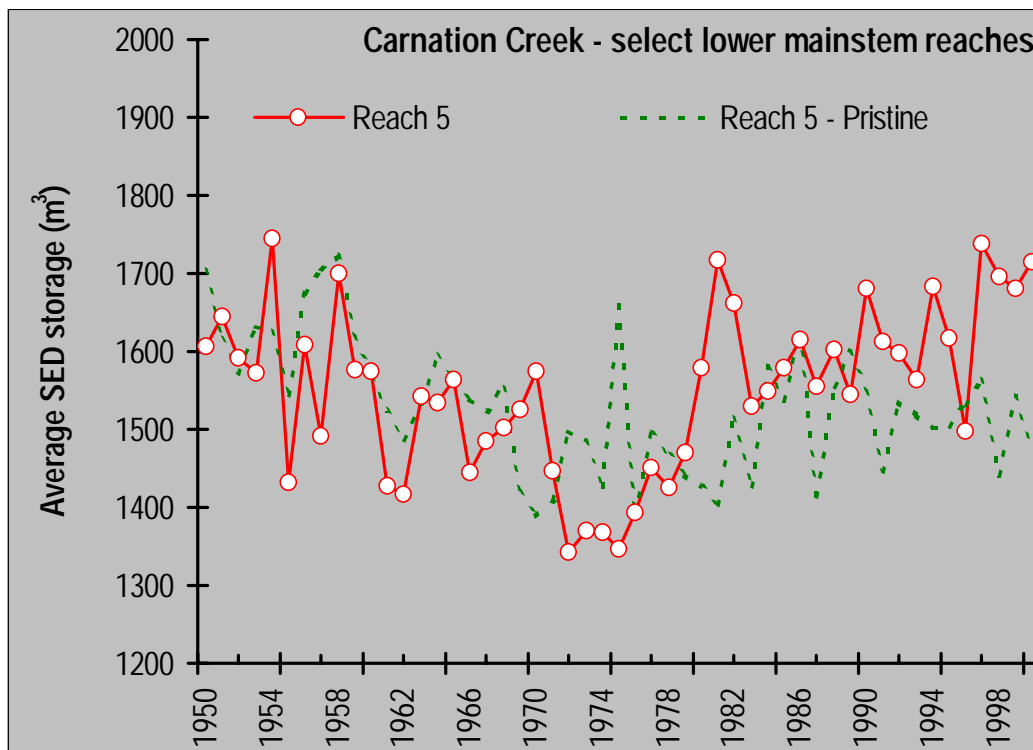
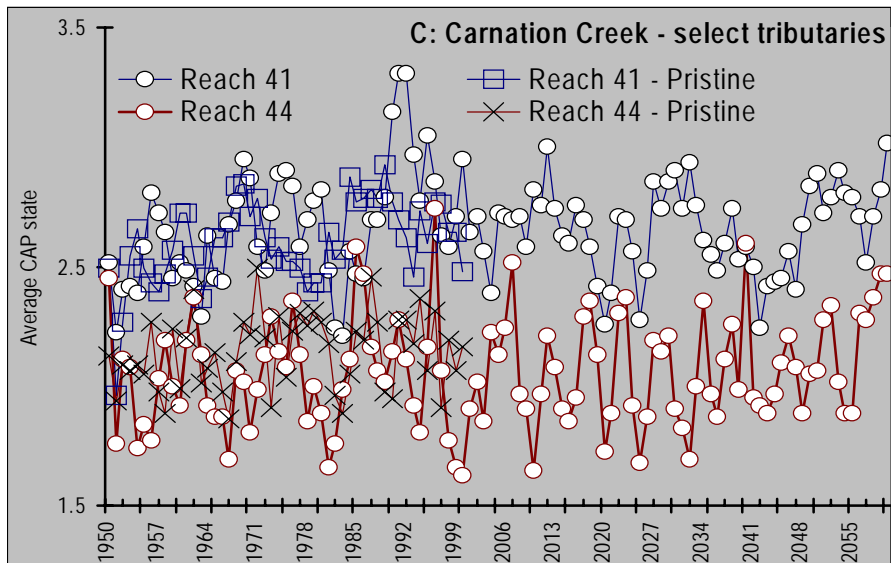
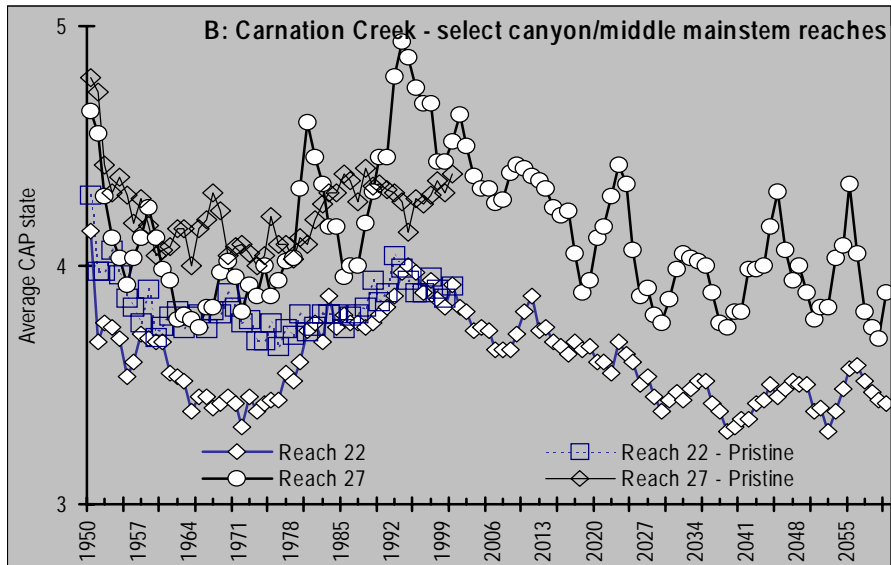
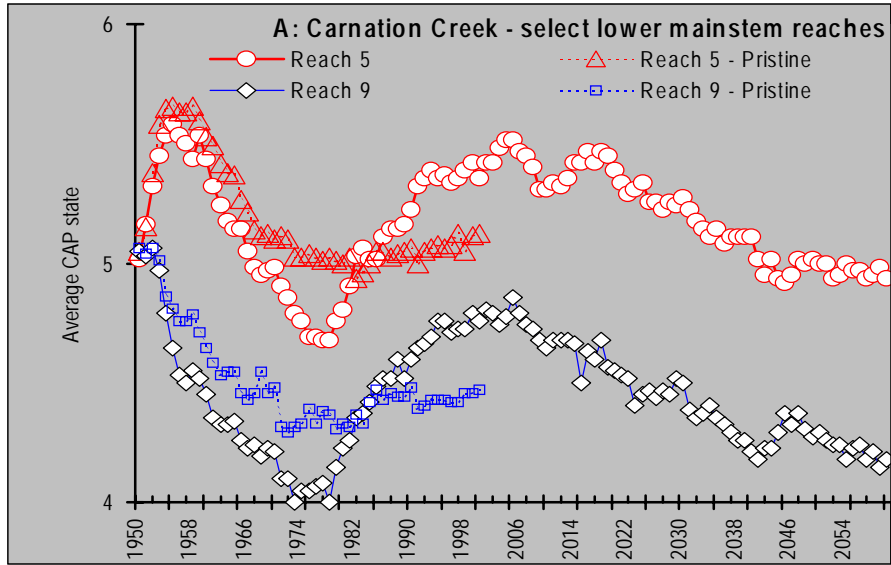


Figure 18: Simulated average sediment storage volumes from 1950 to 2000 for reach 5 under pristine conditions (green line) and historical logging (red line).

Figure 19 shows the implications of the sediment storage volumes given in Figure 16 on CAP state. Simulations suggested that the lower mainstem reaches would initially degrade, and then remain aggraded until approximately 2038 when they recovered to their pristine CAP state (Figure 19A). In contrast, the average effect of logging on the upper canyon section of Carnation Creek tended to be degradation (Figure 19B). In the selected tributaries, logging did not produce any significant change in CAP states over the pristine base case values (Figure 19C).

Considerable levels of year to year variation in average CAP states were observed. Within any given Monte Carlo trial, the variation in CAP state transitions from year to year is even larger. The rapid “flip flopping” from one CAP state to the next suggests that the system is too “flashy” under the current values for parameters and expert rules. Most likely, this can be attributed to the unrealistically large values for annual movement rates for LWD and sediment. The level of year to year variation in these movement rates is likely also too high.

Figure 19 (next page): Simulated average CAP from 1950 to 2060 (historical logging) for select reaches under pristine conditions (unfilled data markers) and historical logging (white filled data markers). CAP state 2 = D2, 3 = D1, 4 = S, 5 = A1, and 6 = A2. The pristine scenario is shown for just 50 years starting in 1950, by which time the CAP state values had stabilized.



3.4 Habitat capability submodel

The average WHC results for coho salmon are given in Figures 20, 21, and 22 for the pristine scenario and the historical logging plan. Two notable observations can be made. First, there was a precipitous drop in WHC in the first 10 years. Second, while the logged scenario produced poorer WHC values between 1976 and 2015, the difference in the logged values and the average WHC values for the pristine scenario were quite small.

The basic cause for the initial decline in WHC appears to be the increase in variability in CAP states that occurs as the simulation progresses combined with the non-linear transformation that the fish habitat relationships apply to the CAP state. At the start of year 1 of a simulation, all reaches in all Monte Carlo runs have a single value for CAP state. As the simulation progresses through time the range of CAP state values for each reach increases. Current parameter values predict a much wider range of possible CAP state values within a few years from the start of the simulation (much higher incidence of reaches ending up in the D3 and A3 states). This is nicely illustrated by Figure 23. Since the fish habitat values are strongly weighted against severely aggraded or degraded reaches, the average habitat values decrease even though the *average* CAP state values stay relatively stable. In effect, the WHC signal became progressively lost over time amidst the CAP state noise even though the negative impacts of logging have increased (Figure 24).

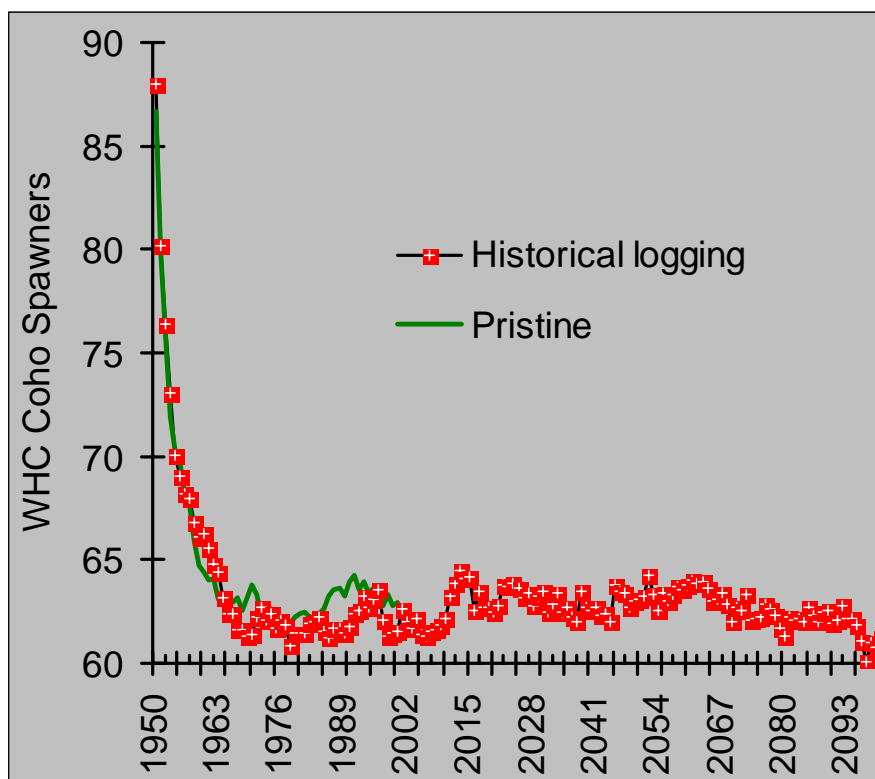


Figure 20: Simulated average WHC values for coho spawning in Carnation Creek under pristine conditions and historical logging activities

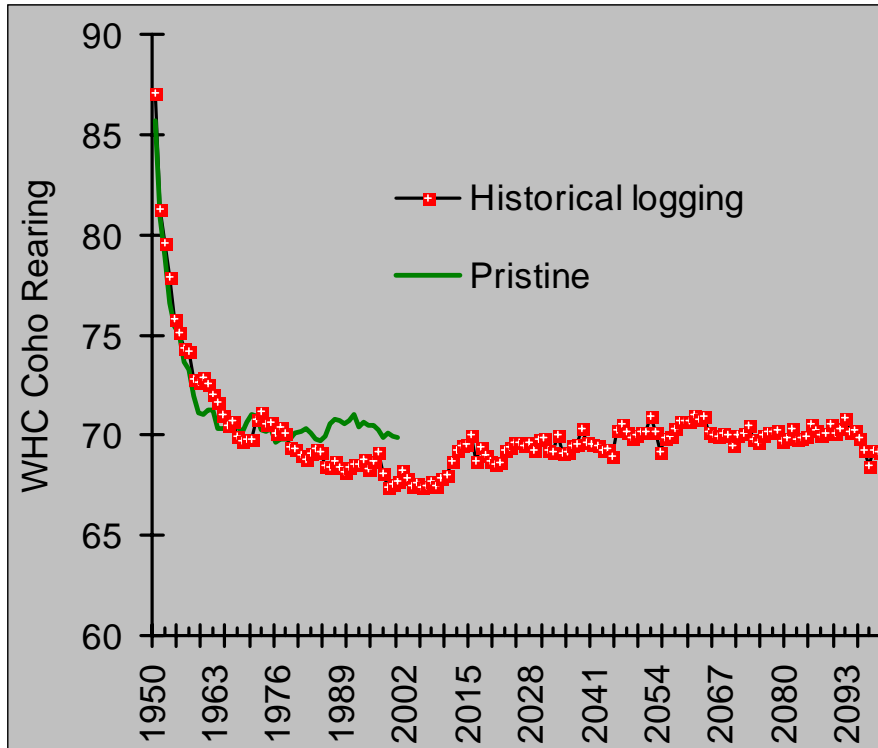


Figure 21: Simulated average WHC values for coho rearing in Carnation Creek under pristine conditions and historical logging activities.

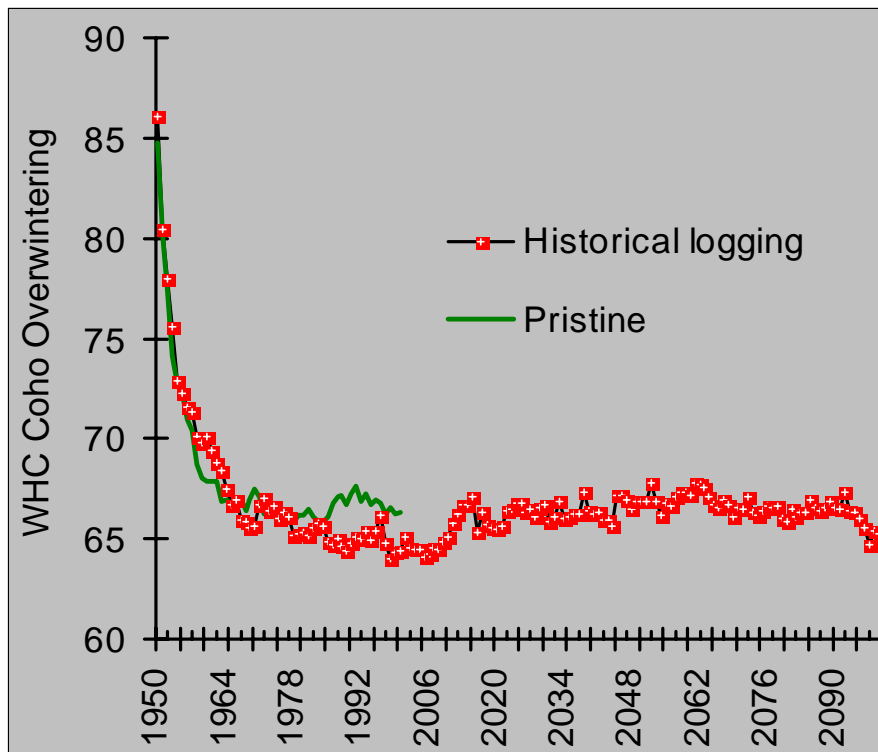


Figure 22: Simulated average WHC values for coho overwintering in Carnation Creek under pristine conditions and historical logging activities.

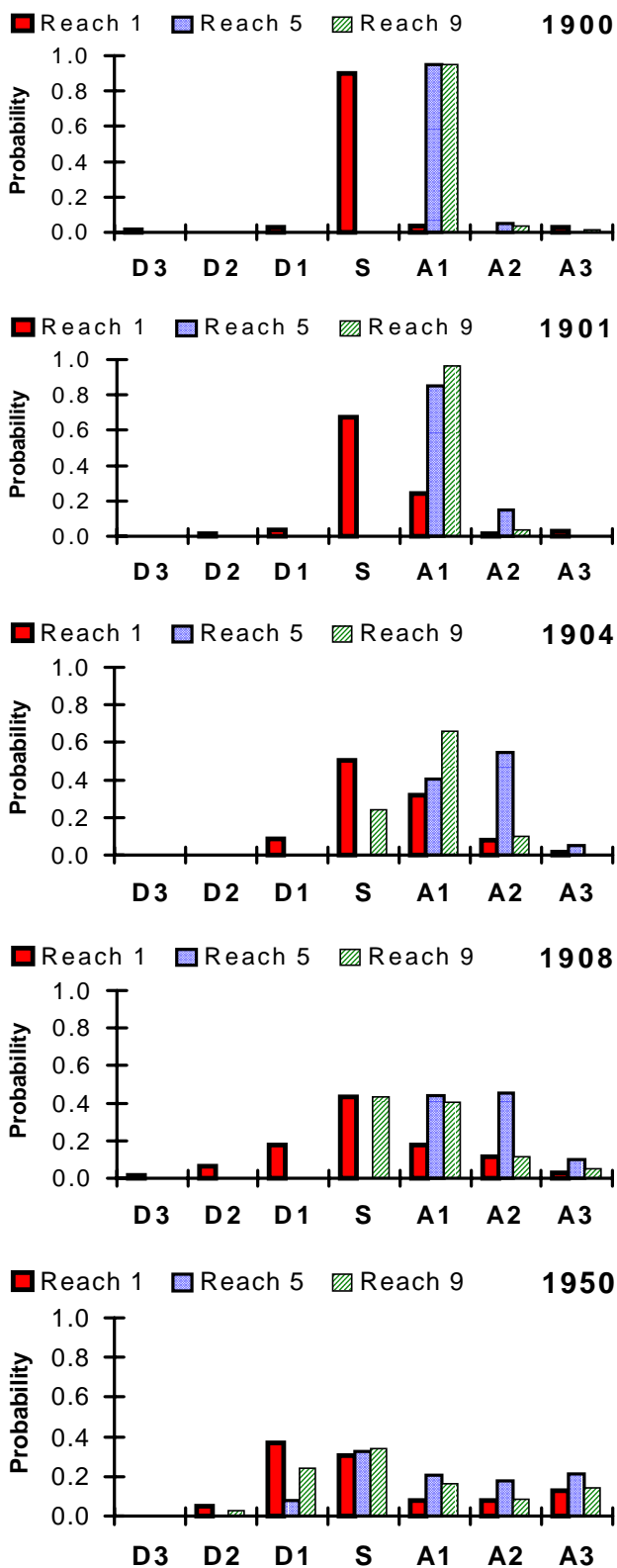


Figure 23: Monte Carlo probability distributions of CAP state for lower mainstem reaches 1, 5, and 9 under pristine conditions and current parameter values. The simulation was started in 1900 and ran until 1950 over 70 Monte Carlo trials.

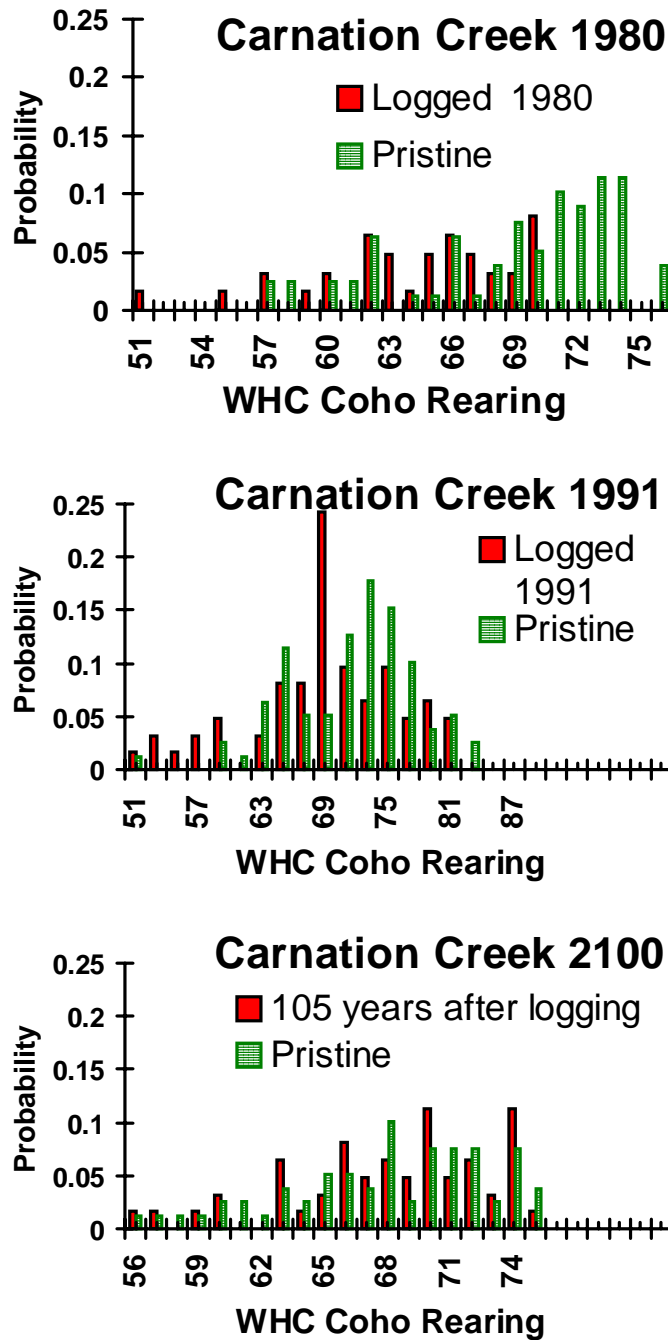


Figure 24: Mean probability distributions of WHC ratings for coho summer rearing under historical logging and pristine conditions (70 Monte Carlo trials). Note the variable x-axis scale.

Viewed at the watershed level, the current model parameters predict a much wider range of CAP state variability than is present at the start of the model run – even without logging. Again, this is presumably due to the LWD and sediment movement rates being too high. As a consequence, the system is moving too rapidly between D3 and A3 CAP states. Lower movement rates would tend to allow the system to better average LWD and sediment inputs and reduce CAP state variability.

Even if the LWD and sediment movement rates were to be reduced, the model may still predict a decline in WHC values unless the initial conditions are set with a reasonable range of CAP state values across reaches. If the model were set up for a pristine scenario with all the reaches in a stable state this problem would still occur (but to a lesser extent). Even in the pristine condition, there will be some distribution of CAP states based on landslide susceptibility (Dan Hogan, BC Ministry of Forests, *pers. comm.*, 1998).

4.0 Conclusion and Recommendations

FFIP-MM now has a structure to integrate the complex chain of processes that links upslope logging activities with distant changes in fish habitat. The model provides a powerful means of exploring these connections through space and time. The results of the preliminary test application of FFIP-MM to Carnation Creek approximated many of the observed trends in LWD and sediment volumes. However, while the direction of the simulated changes was consistent with the observed trends, the magnitudes of the changes were not well reproduced. The differences in simulated and observed conditions are most likely the result of excessively rapid rates of CAP state change (excessive LWD and sediment movement rates). This results in the system being too “flashy”, masking the true magnitude of logging impacts on fish habitat.

Is this a result of the current parameter values or a necessary result of the structure of the model? We believe that it is largely the result of the current parameter values although there may be slight influences by the current model structure. The following suggestions may be useful:

1. Properly parameterize the model’s expert rules by soliciting the input of the appropriate FFIP-MM researchers, then re-run the simulations.
2. Ensure that all runs start out with a reasonable distribution of CAP state values across reaches that reflects the expected level of natural variability. If the system is already in the best state it can be, then future performance will inevitably be worse because there is a chance of it being worse in the future.
3. Review the distributions and parameters used for variability in LWD and sediment movement. At the moment, these are log-normal with variances that may be set too high. However, even when the variances are set rather low, application of a log-normal multiplier to reaches having equilibrium movement rates above 50% to 60% will frequently result in 100% of the LWD or sediment leaving the reach in a single year. A gamma distribution, which models the time required for α random events to occur with a mean time between events of β , may be more appropriate. For example, if we know that a major storm event capable of flushing out all LWD in a reach occurs every 25 years, the two parameter gamma distribution can be used to determine how many years it will take before the next 5 floods flushing events have occurred. Using the existing calibration routine, the values of $FL_{e,r}$ and $FS_{e,r}$ could be used to guide the parameterization of these distributions.
4. Adjust the sediment stored by LWD so that sediment inputs are more closely controlled by LWD dynamics. Consider using non-linear relationships.
5. Re-run the multiple regression analyses conducted by Wise (1997) without the bend angle predictor variable, and use these in the upslope submodel.
6. Ensure that riparian inputs are reasonable – reducing these will reduce LWD movement rates (recall equation 1).
7. Consider using a finer time-step for the channel submodel calculations to reduce numerical instability.

Ultimately, a more formal evaluation strategy must be undertaken. This evaluation strategy should involve further participation by the FFIP-MM research group. We encourage gaming with the model, both independently and jointly, to tune the model to better match both historical data and professional judgements of reasonable qualitative behaviour.

5.0 References

- British Columbia Ministry of Environment.** 1996. *Forest Practices Code of British Columbia: Channel Assessment Procedure Field Guidebook*. Canadian Cataloguing in Publication Data. 97 pp.
- British Columbia Ministry of Environment.** 1995. *Forest Practices Code of British Columbia: Mapping and Assessing Terrain Stability Guidebook*. Canadian Cataloguing in Publication Data. 34 pp.
- ESSA Technologies Ltd.** 1998. FFIP-MM – Fish Forestry Interaction Program Management Model: User’s Guide. Prepared for BC Ministry of Forests by ESSA Technologies Ltd., Vancouver, BC, 46 pp.
- Hartman, G.F., J.C. Scrivener, and M.J. Miles.** 1996. Impacts of logging in Carnation Creek, a high-energy coastal stream in British Columbia, and their implication for restoring fish habitat. *Can. J. Fish. Aquat. Sci.* **53**(Suppl. 1): 237 – 251.
- Hogan, D. L.** 1989. Channel response to mass wasting in the Queen Charlotte Islands, British Columbia: temporal and spatial changes in stream morphology. *incomplete reference: pp. 125-142*.
- Hogan, D.L and J.W. Schwab.** 1990. *Precipitation and Runoff Characteristics, Queen Charlotte Islands*. Land Management Report No. 60, British Columbia Ministry of Forests. Canadian Cataloguing in Publication Data. 46 pp.
- McHenry, M.L., E. Shott, R.H. Conrad, and G.B. Grette.** 1998. Changes in the quantity and characteristics of large woody debris in streams of the Olympic Pininsula, Washington, USA (1982 – 1993). *Can. J. Fish. Aquat. Sci.* **55**: 1395 – 1407.
- Rollerson,** 1992. *Relationships between terrain attributes and post-logging landslide activity: Skidegate Plateau, Queen Charlotte Islands*. Land Management Report No. 76, BC Ministry of Forests. Canadian Cataloguing in Publication Data. 11pp.
- Wise, Michael P.** 1997. *Probabilistic Modelling of Debris Flow Travel Distance Using Empirical Volumetric Relationships*. Masters of Applied Science Thesis. Department of Civil Engineering, University of British Columbia. 274 pp.

Appendix A: Parameter Values Used in the Simulations⁶

Table A1: Riparian Tree Fall parameters.

Model: Riparian Volume (m ³) = $c \times \{(Stand\ Age - lag)/(d - lag) + (Stand\ Age - lag)\}$	
<i>c</i> : Max volume (m ³ .100m stream reach (both banks).year ⁻¹)	0.5
<i>d</i> : Years to ½ maximum riparian LWD contribution	35
<i>lag</i> : Time lag before riparian LWD contributions begin	10 years

Table A2: Proportion of reach volume storing LWD in steady state (equilibrium).

	<i>SPr</i>	<i>SPb</i>	<i>SPb-w</i>	<i>CPb</i>	<i>CPC-w</i>	<i>RPC-w</i>	<i>RPg-w</i>
<i>D3</i>	0.05	0.07	0.09	0.1	0.1	0.12	0.15
<i>S</i>	0.15	0.19	0.2	0.21	0.23	0.25	0.3
<i>A3</i>	0.19	0.2	0.23	0.25	0.28	0.3	0.4

Annual proportion of LWD lost to the atmosphere through natural decay (κ)

$\kappa = 0.0001$

Table A3: Proportion of reach volume storing coarse sediment in steady state (equilibrium).

	<i>SPr</i>	<i>SPb</i>	<i>SPb-w</i>	<i>CPb</i>	<i>CPC-w</i>	<i>RPC-w</i>	<i>RPg-w</i>
<i>D3</i>	0.1	0.1	0.1	0.11	0.15	0.2	0.25
<i>S</i>	0.3	0.3	0.3	0.3	0.3	0.31	0.35
<i>A3</i>	0.35	0.4	0.5	0.5	0.55	0.55	0.55

Table A4: Volume of sediment stored by LWD (Γ).

Model: $\Gamma = a + m \times (\text{proportion reach volume LWD})$	
<i>a</i>	0
<i>m</i>	0.3
proportion reach volume LWD	from Table A2, or using run time values

⁶ *** Note: the model developer arbitrarily assigned values for the expert rules used in the test runs of FFIP-MM. Only the volumetric regression parameters used to calculate the debris slide travel distance and magnitude were based on empirical data.

Table A5: Stand growth parameters as a function of site index.

Model: Volume (m³) = c × Stand Age^m / (d^m + Stand Age^m)				
	<i>0 to 10</i>	<i>11 to 20</i>	<i>21 to 30</i>	<i>31 to 40+</i>
<i>c</i> : Maximum volume (m ³ .ha ⁻¹) for very old stands	500	600	900	1000
<i>d</i> : Years to ½ max. volume	100	90	80	70
<i>m</i> : Curvilinearity in the relationship	2	2	2	2

Table A6: Downed LWD dynamics.

Model: Volume Dead LWD = DeadLWD_(y-1) + NewlyDeadLWD_y × EXP(-Annual decay rate)	
Proportion of standing trees converted to downed LWD upon harvesting	0.2
Annual proportion of new growth added to dead pool	0.02
Annual decay rate of downed LWD	3.25

Table A7: Slope failure hazard classification. “V” = very, “L” = low, “M” = medium, and “H” = high. Column headers represent age categories, while the row labels refer to the five slope stability classes under the BC Ministry of Environment’s terrain stability assessment procedure.**Old Growth:**

Class I	VL
Class II	VL
Class III	VL
Class IV	L
Class V	M

Clear Cut:

	0 to 5	6 to 15	16 to 30	31 to 75	76 to 200	200+
Class I	L	L	VL	VL	VL	VL
Class II	M	M	L	L	VL	VL
Class III	H	M	L	L	L	VL
Class IV	VH	H	M	L	L	L
Class V	VH	VH	H	M	M	M

Roads:

	0 to 5	6 to 10	11 to 15	16 to 20	21 to 25	26+
Class I	VL	L	L	M	L	VL
Class II	L	L	L	M	M	L
Class III	L	L	M	H	M	L
Class IV	L	M	M	VH	VH	L
Class V	M	M	H	VH	VH	L

Gullies:

Class I	M
Class II	H
Class III	H
Class IV	VH
Class V	VH

Table A8: Slope failure probability parameters.

Model: $P(\text{failure}) = c \times (\text{Storm Intensity Multiplier})^m / (d^m + (\text{Storm Intensity Multiplier})^m)$	VL	L	M	H	VH
	c : Maximum probability (ha.yr ⁻¹) for very large storm years (i.e. 99 th percentile of the storm intensity distribution)	0.09	0.095	0.115	0.18
p : Minimum probability (ha.yr ⁻¹) for very small (dry) storm years (i.e. 1 st percentile of the storm intensity distribution)	0.001	0.015	0.025	0.04	0.05
d : Relative storm intensity producing a probability of failure ½ the maximum value	1.25	1.25	1	1	0.75
m : Curvilinearity parameter	1	1.2	1.75	2	2.25

Table A9: Initial slide volume (Vinit) parameters for four terrain classes.

Model: $V_{\text{init}} = c \times (\text{Storm Intensity Multiplier})^m / (d^m + (\text{Storm Intensity Multiplier})^m)$	Clear cut	Road	Gully	Old Growth
	c : Maximum initial slide volume (m ³) for very large storm years (i.e. 99 th percentile of the storm intensity distribution)	4000	800	2500
p : Minimum initial slide volume (m ³) for very small (dry) storm years (i.e. 1 st percentile of the storm intensity distribution)	100	20	10	140
d : Relative storm intensity producing an initial slide volume of ½ the maximum volume	1	1	1	1.7
m : Curvilinearity parameter	0.9	0.5	1	1.25

Table A10: Proportion of LWD entrained by debris slides of different magnitudes

	Small open slope slide	Medium open slope slide	Large open slope slide
Standing (live or rooted) LWD	0	0.15	0.25
Downed (dead) LWD	0.75	0.9	1
Stumps (clear-cut sites)	0	0.6	0.95

Table A11: Total slide volumes corresponding to “small”, “medium”, and “large” magnitude failure events

	Volume (m ³)
Small	≤ 400
Medium	401 to 999
Large	≥ 1000

Table A12: Multipliers used to derive bank input volumes of sediment in aggrading reaches

Model: Bank Input Sediment (m ³) = Net Sediment Input (m ³) x multiplier	
S → A1 multiplier	0.1
A1 → A2 multiplier	0.2
A2 → A3 multiplier	0.3